SGP-TR-97

Transient Pressure Analysis in **Strip** Reservoirs with Linear Skin Discontinuities

Priscilla *G.* McLeroy

January 1986

Financial support was provided through the Stanford Geothermal Program under Department of Energy Contract No. DE-AT03-80SF11459 and by the Department of Petroleum Engineering, Stanford University

Stanford Geothermal Program
Interdisciplinary Research in
Engineering and Earth Sciences
STANFORD UNIVERSITY
Stanford, California

ABSTRACT

Discontinuities in reservoirs are important considerations when analysing pressure drawdown and buildup tests. The changes exhibited in test results can reveal important geometrical features of the reservoir boundary. And, based on the pressure transient analysis, conclusions as to the preferred treatment of the reservoir can be drawn.

A mathematical model of analysing pressure transient tests for linear skin discontinuities is presented. The case of a strip reservoir which is unbounded horizontally in one direction and bounded with impermeable barriers vertically and containing a linear skin discontinuity is proposed. The problem is solved using the two dimensional diffusion equation with successive integral transformations.

Confirmation of the solution is demonstrated by the early time line source pressure response and the late time linear flow pressure response. Application to well testing can be made with superposition of the constant rate fluid production and with matching times to events such as fluid barriers with the solutions.

TABLE OF CONTENTS

ABSTRACT ii

LIST OF FIGURES iv

LIST OF TABLES v

I. INTRODUCTION 1

II. LITERATURE SURVEY 3

III. STATEMENT OF PROBLEM 6

IV. ANALYTICAL, SOLUTION 7

V. DISCUSSION 21

VI. COMPUTATIONAL PROCEDURES 30

VII. CONCLUSIONS AND RECOMMENDATIONS 31

NOMENCLATURE 32

REFERENCES 33

APPENDIX A. DELIMITING SOLUTION FOR LINE SOURCE CONCURRENCE 35

APPENDIX B. COMPUTER PROGRAMS 40

APPENDIX C. SELECTED DATA 53

LIST OF FIGURES

Figure 1 : Schematic diagram for the linear skin discontinuity system 7

Figure 2 : Semilog plot depicting the behavior of the pressure function during numerical inversion 22

Figure 3 : Logarithmic plot of p_D vs. t_D for values generated at $y°_D = 20$ in the Fourfirst and Stehfirst **Programs** 23

Figure 4 : Logarithmic plot of the sum of line sources with a well located in the center of the system. $p_D = \frac{1}{2}\sum_{i=1}^{\infty} Ei\left(-\frac{y°_{Dj}^2}{4t_D}\right) - \frac{1}{2} Ei\left(-\frac{1}{4t_D}\right)$ where $y°_D$ ranges from 10 to 10000 25

Figure 5 : Logarithmic plot of p_D vs. t_D for composite reservoir with $y°_D$ varying from 10 to 200 26

Figure 6 : Logarithmic plot of p_D vs. t_D shifted data from the composite system. 27

Figure 7 : Logarithmic plot for case of infinite and zero boundary skin 28

Figure 8 : Logarithmic plot for case of infinite and unit mobility 29

Figure 9 : Flowchart for Fourfirst **Program** 41

Figure 10 : Flowchart for Stehfirst Pro**gram** 47

LIST OF TABLES

Table C-1 : Selected Data from Stehfirst and Fourfirst Program Evaluation.....54

Table C-2 : Selected Data from Composite Reservoir -- Nonshifted 55

Table C-3 : Selected Data from Composite Reservoir -- Shifted..... 56

Table C-4 : Selected Data for Varying Mobility Ratios and Skin..... 57

Table C-5 : The Line Source Solution..... 58

ABSTRACT

Discontinuities in reservoirs are important considerations when analysing pressure drawdown and buildup tests. The changes exhibited in test results can reveal important geometrical features of the reservoir boundary. And, based on the pressure transient analysis, conclusions as to the preferred treatment of the reservoir can be drawn.

A mathematical model of analysing pressure transient tests for linear skin discontinuities is presented. The case of a strip reservoir which is unbounded horizontally in one direction and bounded with impermeable barriers vertically and containing a linear skin discontinuity is proposed. The problem is solved using the two dimensional diffusion equation with successive integral transformations.

Confirmation of the solution is demonstrated by the early time line source pressure response and the late time linear flow pressure response. Application to well testing can be made with superposition of the constant rate fluid production and with matching times to events such as fluid barriers with the solutions.

TABLE OF CONTENTS

ABSTRACT ii

LIST OF FIGURES iv

LIST OF TABLES v

I. INTRODUCTION 1

II. LITERATURE SURVEY 3

III. STATEMENT OF PROBLEM 6

IV. ANALYTICAL SOLUTION 7

V. DISCUSSION 21

VI. COMPUTATIONAL PROCEDURES 30

VII. CONCLUSIONS AND RECOMMENDATIONS 31

NOMENCLATURE 32

REFERENCES 33

APPENDIX A. DELIMITING SOLUTION FOR LINE SOURCE CONCURRENCE ...35

APPENDIX B. COMPUTER PROGRAMS 40

APPENDIX C. SELECTED DATA 53

LIST OF FIGURES

Figure 1 : Schematic diagram for the linear skin discontinuity system 7

Figure 2 : Semilog plot depicting the behavior of the pressure function during numerical inversion. 22

Figure 3 : Logarithmic plot of p_D vs. t_D for values generated at $y^\circ_D = 20$ in the Fourfirst and Stehfirst Programs. 23

Figure 4 : Logarithmic plot of the sum of line sources with a well located in the center of the system. $p_D = -\frac{1}{2}\sum_{j=1}^{\infty} Ei\left(-\frac{y^{\circ 2}_D j^2}{4t_D}\right) - \frac{1}{2} Ei\left(-\frac{1}{4t_D}\right)$ where y°_D ranges from 10 to 10000. 25

Figure 5 : Logarithmic plot of p_D vs. t_D for composite reservoir with y°_D varying from 10 to 200. 26

Figure 6 : Logarithmic plot of p_D vs. t_D shifted data from the composite system. 27

Figure 7 : Logarithmic plot for case of infinite and zero boundary skin. 28

Figure 8 : Logarithmic plot for case of infinite and unit mobility. 29

Figure 9 : Flowchart for Fourfirst Program 41

Figure 10 : Flowchart for Stehfirst Program 47

LIST OF TABLES

Table C-1 : Selected Data from Stehfirst and Fourfirst Program Evaluation 54

Table C-2 : Selected Data from Composite Reservoir ... Nonshifted 55

Table C-3 : Selected Data from Composite Reservoir ... Shifted 56

Table C-4 : Selected Data for Varying Mobility Ratios and Skin 57

Table C-5 : The Line Source Solution 58

I. INTRODUCTION

Pressure transient theory has been classically based on reservoir homogeneity. However, practice has shown that it is quite important to consider heterogeneities and their effect on transient pressure behavior. Heterogeneities such as natural fractures, faults, gas caps, and man-made anomalies such as hydraulic fractures or injection well tests exemplify alterations in transient pressure behavior. In order to understand such anomalies, pressure buildup and drawdown tests have become valuable resources for explaining drainage limits, formation and wellbore storage, average permeability, and the presence of flow discontinuities.

In recent years, flow barriers have attracted industry and academic research interest. Areas such as the North Slope of Alaska which exhibits a highly faulted structure, in addition to a major gas cap, and the tight sands of Colorado which contain hydraulic fractures typify complex discontinuities in reservoir structure. Notwithstanding educationdl interests are economical interests at stake in producing these fields. As a result, more information is being demanded from well tests such that reservoir development can be planned from strategy rather than conjecture. Alternately, research has the challenge to establish theoretical bases in pressure transient work for defining fluid behavior with internal flow barriers.

Studies concerning flow discontinuities have centered on internal circular and linear boundaries with either constant pressure and no flow or constant rate systems. Linear boundaries have been analysed quite extensively with assumptions of a constant change in pressure and constant mobility across the boundary. In work to date, the concept of a system with a penetrable flow boundary compounded with a skin has not been analysed. This type of system would apply to reservoirs exhibiting the heterogeneities described earlier. For example, the gas cap showing high compressibility compared to the otherwise uniform formation compressibility may produce a discontinuity with skin.

The research presented in this paper involves a semi-infinite reservoir with a line source well located some distance from a linear skin discontinuity. Constant rate fluid production is

assumed. The pressure drop associated with the skin will be a function of the flow rate and change in pressure as established from behavior of the line source near the discontinuity. Measurement of the skin with varying distances along the linear boundary from the line source provides data to construct type curves.

II. LITERATURE SURVEY

Since the late 1940's attention has been given to the use of transient pressure measurements in wells as a device to investigate the behavior of aquifers and petroleum reservoirs. Theoretically, pressure buildup and drawdown results describe the nature of the system from whence they are drawn. Results, based on the soundness of this theory, are then made the basis for developing reservoir description. The assessment of buildup and drawdown tests have focused on two general conditions: constant pressure boundaries and/or no-flow boundaries. The research presented in this paper considers a semi-infinite, constant rate reservoir containing a linear skin discontinuity; the skin being a result of changes in fluid properties caused by fluid-fluid interfaces or structural discontinuities.

In a classic text by *Carslaw and Jaeger* [1959], the solution for a constant flow rate line source well inside an infinite reservoir was presented. *Van Everdingen and Hurst* [1949] applied the Laplace transformation to this condition and showed the solution for a finite radius well in an infinite system. The line source referred to in these papers is defined by *Ramey, Kumar, and Gulati* [1973] as a well having a vanishing radius in an infinitely large system. The formation is considered at constant permeability, porosity, and thickness while the fluid iq considered producing at a constant rate with constant compressibility and viscosity. Also, pressure gradients are small such that the square of the gradient may be neglected in the flow system. *Matthews and* Russell [1967], among others, define the infinite reservoir as an infinite-acting reservoir where there is negligible pressure depletion at the outer boundary caused by a well located some distance from that boundary.

Completing the reservoir definition calls for understanding the internal boundaries, if they exist. As described by *Muskat* [1937], inner discontinuities are of practical interest when abrupt changes in permeability are noticed with respect to geometrical boundary crossover. Muskat also showed two conditions that must be satisfied when considering discontinuities: equal pressures continuing across the surface of discontinuity and, based on Darcy's Law, the normal

velocity also continuous across the discontinuity. As a result, the pressure regime will correspond to a composite flow system where the two varying permeability regions are connected physically and geometrically. ***Bixel, Larkin, and van Poollen*** **[1963]** presented a general analysis of the linear discontinuity in an infinite system. Mathematically, they described two regions with independently homogeneous fluid and rock properties. ***Bixel, et al.*** extended ***Muskat's*** assumptions and developed a method for measuring pressure changes at producing wells some distance, which they also calculated, from the discontinuity. Others, such as ***Standing*** **[1964]**, ***Gibson and Campbell*** **[1970]**, ***Prasad*** **[1975]**, ***Fenske*** **[1984]**, and ***Yaxley*** **[1985]** developed supporting results for calculating distance to a discontinuity.

The concept of measuring the pressure effects on a well from an inner boundary have been studied by numerous authors. ***Elkins and Skov*** **[1960]** used the approach of an anisotropic media containing natural fractures and correlated results from pressure transient curves to injection tests with good agreement. Similarly, ***Cinco, Samaniego, and Dominguez*** **[1976]** studied the natural fracture effect on transient pressure but treated the fracture as an internal finite linear boundary. ***Davis and Hawkins*** **[1963]** looked at another form of internal boundary when they studied effects on pressure transients near a fault, (no-flow boundary). ***Hurst*** **[1960]** considered the interference between oil fields similar to that of a well being affected by some other fluid producer. In *Hurst's* discussion, it is shown that the pressure drop occurring at a distance, r, is dependent upon the physical parameters existing in the formation at that point. In essence, interference seen in the subject well is accounted for via two parameters, distance ret moved and rate of voidage, q', with other formation parameters such as thickness and permeability held constant. As developed earlier, ***Hurst*** **[1960]** simplified the complexities formerly associated with identifying and determining reservoir pressure in the material balance relationship by treatment with the Laplace transformation. The inversion of which showed pressure as an explicit function of those factors contributing to its change.

Horner **[1951]**; ***Matthews, Brons, and Hazebroek*** **[1954]**; ***Collins*** **[1961]**; and, ***Earlougher, Ramey, Miller, and Mueller*** **[1968]** used the method of images for generating the

effects of linear boundaries. *Stallman* [1952] and Tiub *and Kumar* [1980] generated log-log type curves based on behavior from imaged source-sink wells generating the effects of both constant pressure and no-flow linear boundaries. Internal circular discontinuities have been studied by *Sageev* [1983]. Results from this study show a well produced near a no-flow boundary developing two different pressure regions. One region, containing the producer displaying; a pressure drop higher than the line source and the other region showing a pressure drop lower than the line source.

The method of images cannot be applied to this problem since the linear skin discontinuity contains neither a constant pressure nor a no-flow boundary. In this research, a permeable skin discontinuity is studied. As such, the approach is similar to the mathematical method developed by *Bixel, et al.* [1963] with variations to their inner boundary condition to include the effect of skin. Also, the method of *Goode and Thambymayagam* [1985] is used where a set of equations describing transient pressure in horizontal wells were derived using successive integral transformations.

III. STATEMENT OF PROBLEM

The objective of this research involves mathematically defining transient pressure in a strip reservoir with a linear skin discontinuity. The characteristics of the skin are measured in relation to a line source well located some fixed distance from the discontinuity. Results from the research provide a basis in transient testing for detecting a semi-permeable discontinuity caused by rock changes or fluid interfaces.

IV. ANALYTICAL SOLUTION

The problem is posed in two dimensions as a strip with a linear skin discontinuity approximated by a vertical plane. An infinite conductivity well is located in region I which produces a fluid of constant compressibility. The initial reservoir pressure is constant Transport of fluids vertically is prohibited and unlimited horizontally, (see figure! 1).

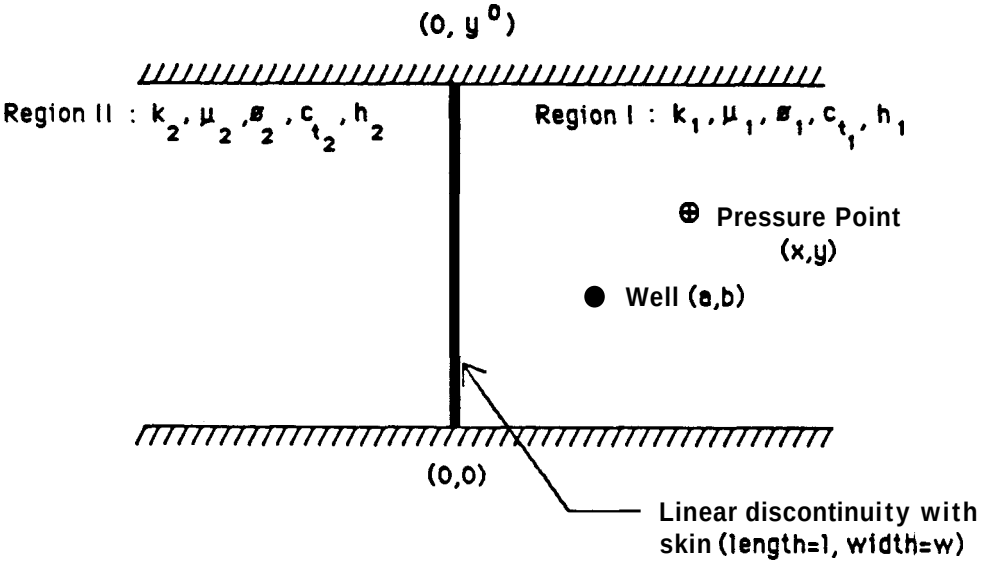

Figure 1 : Schematic diagram for the linear skin discontinuity system

The diffusivity, η, and mobility, λ, are defined for each region as:

$$\eta_1 = \left[\frac{k}{\phi\mu c_t}\right]_1 \qquad \lambda_1 = \left[\frac{k}{\mu}\right]_1$$

$$\eta_2 = \left[\frac{k}{\phi\mu c_t}\right]_2 \qquad \lambda_2 = \left[\frac{k}{\mu}\right]_2$$

The partial differential equations governing the isothermal fluid flow are as follows:

For the first region, ($x>0$), containing the active constant rate well,

$$\frac{\partial p_1}{\partial t} = \eta_1 \left[\frac{\partial^2 p_1}{\partial x^2} + \frac{\partial^2 p_1}{\partial y^2} \right] + \frac{\eta_1}{\lambda_1} q(t)\delta(x-a)\delta(y-b) \tag{1}$$

For the second region, (x<0),

$$\frac{\partial p_2}{\partial t} = \eta_2 \left[\frac{\partial^2 p_2}{\partial x^2} + \frac{\partial^2 p_2}{\partial y^2} \right] \tag{2}$$

The inital, boundary, and interface conditions for the problem are:

Initial Conditions:

$$p_1(x,y,0) = \text{Pi} \tag{3}$$

$$p_2(x,y,0) = p_i \tag{4}$$

Boundary Conditions:

$$p_1(\infty,y,t) = p_2(-\infty,y,t) = p_i \tag{5}$$

For x>0, x<0 :

$$\frac{\partial p_1}{\partial y}\Big]_{y^o} = \frac{\partial p_1}{\partial y}\Big]_0 = \frac{\partial p_2}{\partial y}\Big]_{y^o} = \frac{\partial p_2}{\partial y}\Big]_0 = 0 \tag{6}$$

Interface Conditions:

$$\left[\lambda \frac{\partial p}{\partial x}\right]_1 = \left[\lambda \frac{\partial p}{\partial x}\right]_2 \tag{7}$$

and for the skin discontinuity,

$$\frac{\partial p_1(0,y,t)}{\partial x} = \frac{-1}{sl}\left[- p_2(0,y,t) + p_1(0,y,t) \right] \tag{8}$$

with, l=1, a characteristic length

To facilitate solution of the problem, dimensionless variables are defined and substituted into the partial differential equations and boundary conditions.

Dimensionless Variables:

$$p_{D_1} = \frac{k_1 h}{\mu_1 q}\left[p_i - p(x,y,t)\right] \tag{9}$$

$$p_{D_2} = \frac{k_2 h}{\mu_2 q}\left[p_i - p(x,y,t)\right] \tag{10}$$

$$x_D = \frac{x}{r_w} \tag{11}$$

$$y_D = \frac{y}{r_w} \tag{12}$$

$$t_D = t_{D_1} = \frac{k}{\phi\mu c_t}\Big]_1 \frac{t}{r_w^2} \tag{13}$$

Dimensionless Equations:

For $x_D > 0$:

$$\frac{\partial p_{D_1}}{\partial t_D} = \frac{\partial^2 p_{D_1}}{\partial x_D^2} + \frac{\partial^2 p_{D_1}}{\partial y_D^2} - \delta(x_D - a)\delta(y_D - b) \tag{14}$$

For $x_D < 0$:

$$\frac{\eta_1}{\eta_2}\frac{\partial p_{D_2}}{\partial t_D} = \frac{\partial^2 p_{D_2}}{\partial x_D^2} + \frac{\partial^2 p_{D_2}}{\partial y_D^2} \tag{15}$$

where t_D is defined in terms of regions I permitting a diffusivity relation between region I and II.

Dimensionless Boundary Conditions:

initial conditions:

$$p_{D_1}(x_D,y_D,0) = 0 \tag{16}$$

$$p_{D_2}(x_D,y_D,0) = 0 \tag{17}$$

outer boundary conditions:

$$p_{D_1}(\infty,y_D,t_D) = p_{D_2}(-\infty,y_D,t_D) = 0 \tag{18}$$

For $x_D > 0$, $x_D < 0$:

$$\left.\frac{\partial p_{D_1}}{\partial y_D}\right]_{y_D^\circ} = \left.\frac{\partial p_{D_1}}{\partial y_D}\right]_0 = \left.\frac{\partial p_{D_2}}{\partial y_D}\right]_{y_D^\circ} = \left.\frac{\partial p_{D_2}}{\partial y_D}\right]_0 = 0 \tag{19}$$

Interface Conditions:

$$\frac{\partial p_{D_1}}{\partial x_D}(0,y_D,t_D) = \frac{\lambda_2}{\lambda_1}\frac{\partial p_{D_2}}{\partial x_D}(0,y_D,t_D) \tag{20}$$

and,

$$\frac{\partial p_{D_1}}{\partial x_D}(0,y_D,t_D) = \frac{-1}{s}\left[-p_{D_2}(0,y_D,t_D) + p_{D_1}(0,y_D,t_D)\right] \tag{21}$$

The next step in solving the problem is with a transformation in time and in the y coordinate,

the variable transform for y_D is defined as,

$$Y_D = \frac{\pi y_D}{y^\circ_D} = \nu y_D \tag{22}$$

where

$$\nu = \frac{A}{y^\circ_D} \tag{23}$$

From *Churchill* [1944], the Laplace transformation in time is defined as,

$$L\left\{F(t)\right\} = \int_0^\infty e^{-St}F(t)dt = f(S) = \bar{f}(S) \tag{24}$$

and from *Selby* [1970], the Finite Fourier Cosine transformation in y,

$$F\left\{G(y)\right\} = \int_0^\pi G(y)\cos(my)\,dy \tag{25}$$

giving the dimensionless pressure to be evaluated as,

$$\bar{\bar{p}}_D = \int_0^{y_D} \cos(my_D) \int_0^\infty e^{-St_D} p_D(x_D,y_D,t_D)\,dt_D dy_D \tag{26}$$

or, more simply as,

$$\bar{\bar{p}}_D = \int_0^{y_D} \cos(my_D)\bar{p}_D\,dy_D \tag{27}$$

applying the Laplace transformation to equation 14 and 15 yields,

for $x_D > 0$:

$$\frac{\partial^2 \bar{p}_{D_1}}{\partial x_D^2} + \nu^2 \frac{\partial^2 \bar{p}_{D_1}}{\partial Y_D^2} - \frac{\delta(x_D-a)\delta(\frac{1}{\nu}Y_D-b)}{S} = S\bar{p}_{D_1} - p_{D_1}(t_D=0) \tag{28}$$

applying the initial condition, equation 16, gives,

$$\frac{\partial^2 \bar{p}_{D_1}}{\partial x_D^2} + \nu^2 \frac{\partial^2 \bar{p}_{D_1}}{\partial Y_D^2} - \frac{\delta(x_D-a)\delta(\frac{1}{\nu}Y_D-b)}{S} = S\bar{p}_{D_1} \tag{29}$$

for $x_D < 0$,

$$\frac{\partial^2 \bar{p}_{D_2}}{\partial x_D^2} + \nu^2 \frac{\partial^2 \bar{p}_{D_2}}{\partial Y_D^2} = \frac{\eta_1}{\eta_2} S\bar{p}_{D_2} - p_{D_2}(t_D=0) \tag{30}$$

applying the initial condition, equation 17, gives,

$$\frac{\partial^2 \bar{p}_{D_2}}{\partial x_D^2} + \nu^2 \frac{\partial^2 \bar{p}_{D_2}}{\partial Y_D^2} = \frac{\eta_1}{\eta_2} S\bar{p}_{D_2} \tag{31}$$

Laplace transforming the boundary conditions,

$$\bar{p}_{D_1}(\infty, y_D, S) = \bar{p}_{D_2}(-\infty, y_D, S) = 0 \tag{32}$$

$$\left.\frac{\partial \bar{p}_{D_1}}{\partial y_D}\right]_{y_D^o} = \left.\frac{\partial \bar{p}_{D_1}}{\partial y_D}\right]_0 = \left.\frac{\partial \bar{p}_{D_2}}{\partial y_D}\right]_{y_D^o} = \left.\frac{\partial \bar{p}_{D_2}}{\partial y_D}\right]_0 = 0 \tag{33}$$

and, Laplace transforming the interface conditions,

$$\frac{\partial \bar{p}_{D_1}}{\partial x_D}(0, y_D, S) = \frac{\lambda_2}{\lambda_1} \frac{\partial \bar{p}_{D_2}}{\partial x_D}(0, y_D, S) \tag{34}$$

$$\frac{\partial \bar{p}_{D_1}}{\partial x_D}(0, y_D, S) = \frac{-1}{s}\left[-\bar{p}_{D_2}(0, y_D, S) + \bar{p}_{D_1}(0, y_D, S)\right] \tag{35}$$

Applying the Finite Fourier Cosine transformation and using the outer bodndary condition, equation 33, to equations 29 and 31,

$$\frac{d^2 \bar{\bar{p}}_{D_1}}{dx_D^2} - \bar{\bar{p}}_{D_1}(\nu^2 m^2 + S) = \frac{\delta(x_D - a)\cos(mb\nu)}{S} \qquad , x_D > 0 \tag{36}$$

$$\frac{d^2 \bar{\bar{p}}_{D_2}}{dx_D^2} - \bar{\bar{p}}_{D_2}(\nu^2 m^2 + \frac{\eta_1}{\eta_2} S) = 0 \qquad , x_D < 0 \tag{37}$$

The Finite Fourier Cosine transformation of the boundary conditions yield,

$$\bar{\bar{p}}_{D_1}(\infty,m,S) = \bar{\bar{p}}_{D_2}(-\infty,m,S) = 0 \tag{38}$$

The Finite Fourier Cosine transformation of the interface conditions yields,

$$\frac{d\bar{\bar{p}}_{D_1}}{dx_D}(0,m,S) = \frac{\lambda_2}{\lambda_1}\frac{d\bar{\bar{p}}_{D_2}}{dx_D}(0,m,S) \tag{39}$$

$$\frac{d\bar{\bar{p}}_{D_1}}{dx_D}(0,m,S) = \frac{-1}{s}\left[-\bar{\bar{p}}_{D_2}(0,m,S) + \bar{\bar{p}}_{D_1}(0,m,S)\right] \tag{40}$$

the General Solution to equation 37 is:

$$\bar{\bar{p}}_{D_2} = Ce^{-\sqrt{v^2m^2+\frac{\eta_1}{\eta_2}S}\,x_D} + De^{\sqrt{v^2m^2+\frac{\eta_1}{\eta_2}S}\,x_D} \qquad ,x_D<0 \tag{41}$$

To find the constant, C, equation 38 will be used.

$$\bar{\bar{p}}_{D_2}(-\infty,m,S) = 0$$

yielding

$$C = 0 \tag{42}$$

Rewriting the general solution,

$$\bar{\bar{p}}_{D_2} = De^{\sqrt{v^2m^2+\frac{\eta_1}{\eta_2}S}\,x_D} \qquad ,x_D<0 \tag{43}$$

To solve equation 36, we take the Laplace transformation with respect to x_D where "u" is the Laplace variable.

defining the following substitutions:

$$\alpha_1 = \nu^2 m^2 + S \tag{44}$$

$$\alpha_2 = \nu^2 m^2 + \frac{\cdot 11}{\bar{1}12} S \tag{45}$$

$$\alpha_3 = \frac{\cos(\nu m b)}{S} \tag{46}$$

Equation 36 becomes:

$$u\,(\,u\bar{\bar{p}}_{D_1} - \bar{\bar{p}}_{D_1}(s,m,x_D{=}0)) - \frac{d\bar{\bar{p}}_{D_1}}{dx_D}\,(s,m,x_D{=}0) - \alpha_1\bar{\bar{p}}_{D_1} = \alpha_3 e^{-au} \tag{47}$$

and, rearranging, equation 47 gives,

$$\bar{\bar{p}}_{D_1} = \frac{\alpha_3 e^{-au} + u\bar{\bar{p}}_{D_1}(x_D{=}0) + \bar{\bar{p}}'_{D_1}(x_D{=}0)}{u^2 - \alpha_1} \tag{48}$$

simplifying,

$$\bar{\bar{p}}_{D_1} = \frac{\alpha_3 e^{-au}}{u^2 - \alpha_1} + \frac{u\bar{\bar{p}}_{D_1}(x_D{=}0)}{u^2 - \alpha_1} + \frac{\bar{\bar{p}}'_{D_1}(x_D{=}0)}{u^2 - \alpha_1} \tag{49}$$

From *Churchill* [1944], inversion of the following Laplace transforms are defined as,

$$L^{-1}\left[\,e^{-au}\,\right] = \delta(x_D{-}a) \tag{50}$$

$$L^{-1}\left[\,\frac{u}{u^2{-}\alpha_1}\,\right] = \cosh(\sqrt{\alpha_1}x_D) \tag{51}$$

and,

$$L^{-1}\left[\frac{1}{u^2-\alpha_1}\right] = \frac{1}{\sqrt{\alpha_1}}\sinh(\sqrt{\alpha_1}x_D) \tag{52}$$

by the Convolution Integral from *Kaplan* [1981],

$$L^{-1}\left[\frac{e^{-as}}{u^2-\alpha_1}\right] = \frac{1}{\sqrt{\alpha_1}}\int_0^{x_D}\delta(z-a)\sinh(\sqrt{\alpha_1}(x_D-z))\,dz \tag{53}$$

Evaluating equation 53 for $x_D<a$ gives,

$$\frac{1}{\sqrt{\alpha_1}}\int_0^{x_D}\delta(z-a)\sinh(\sqrt{\alpha_1}(x_D-z))\,dz = 0 \tag{54}$$

and for $x_D>a$,

$$\frac{1}{\sqrt{\alpha_1}}\int_0^{x_D}\delta(z-a)\sinh(\sqrt{\alpha_1}(x_D-z))\,dz = \frac{1}{\sqrt{\alpha_1}}\sinh(\sqrt{\alpha_1}(x_D-a)) \tag{55}$$

Application of the inverse Laplace transformation to equation 49 yields:

For $0<x_D<a$,

$$\bar{\bar{p}}_{D_1} = \bar{\bar{p}}_{D_1}(x_D=0)\cosh(\sqrt{\alpha_1}x_D) + \bar{\bar{p}}'_{D_1}(x_D=0)\frac{1}{\sqrt{\alpha_1}}\sinh(\sqrt{\alpha_1}x_D) \tag{56}$$

and if $x_D>a$,

$$\bar{\bar{p}}_{D_1} = \frac{\alpha_3}{\sqrt{\alpha_1}}\sinh(\sqrt{\alpha_1}(x_D-a)) + \bar{\bar{p}}_{D_1}(x_D=0)\cosh(\sqrt{\alpha_1}x_D) + \bar{\bar{p}}'_{D_1}(x_D=0)\frac{1}{\sqrt{\alpha_1}}\sinh(\sqrt{\alpha_1}x_D) \tag{57}$$

Solving the problem defined in region 11, $x_D<0$, is done by evaluation of the general solution obtained in equation 43.

Recall equation 43,

$$\bar{\bar{p}}_{D_2} = De^{\sqrt{\alpha_2}\, x_D} \qquad ; x_D<0$$

then differentiate with respect to x_D giving,

$$\frac{d\bar{\bar{p}}_{D_2}}{dx_D} = D\sqrt{\alpha_2}e^{\sqrt{\alpha_2}\, x_D} \tag{58}$$

Substituting equation 58 into 39 at x_D=0 gives,

$$\frac{d\bar{\bar{p}}_{D_1}}{dx_D}(0,m,S) = \frac{\lambda_2}{\lambda_1}D\sqrt{\alpha_2} \tag{59}$$

and, similarly, substituting equation 58 into equation 40 at x_D=0 gives,

$$\frac{\lambda_2}{\lambda_1}D\sqrt{\alpha_2} = \frac{-1}{s}\left[-D + \bar{\bar{p}}_{D_1}(0,m,S)\right] \tag{60}$$

rearranging equation 60 yields,

$$\bar{\bar{p}}_{D_1}(0,m,S) = D\left[1 - s\frac{\lambda_2}{\lambda_1}\sqrt{\alpha_2}\right] \tag{61}$$

Substituting equations 59 and 61 into equation 57 gives,

$$\bar{\bar{p}}_{D_1} = \frac{\alpha_3}{\sqrt{\alpha_1}}\left[\frac{e^{\sqrt{\alpha_1}\,(x_D-a)} - e^{-\sqrt{\alpha_1}\,(x_D-a)}}{2}\right]$$

$$+ D\left[1 - s\frac{\lambda_2}{\lambda_1}\sqrt{\alpha_2}\right]\left[\frac{e^{\sqrt{\alpha_1}\, x_D} + e^{-\sqrt{\alpha_1}\, x_D}}{2}\right]$$

$$+ D\frac{\lambda_2}{\lambda_1}\frac{\sqrt{\alpha_2}}{\sqrt{\alpha_1}}\left[\frac{e^{\sqrt{\alpha_1}\, x_D} - e^{-\sqrt{\alpha_1}\, x_D}}{2}\right] \tag{62}$$

Applying equation 38 and rearranging,

$$D = \frac{-\frac{\alpha_3}{\sqrt{\alpha_1}} e^{-\sqrt{\alpha_1}\, a}\left[\frac{e^{\sqrt{\alpha_1}\, x_D} - }{2}\right]}{f + g} \tag{63}$$

where f and g are defined as,

$$f = \frac{1}{2}\left[1 - s\frac{\lambda_2}{\lambda_1}\sqrt{\alpha_2}\right]\left[\frac{e^{\sqrt{\alpha_1}\, x_D} + e^{-\sqrt{\alpha_1}\, x_D}}{2}\right] \tag{64}$$

and

$$g = \frac{\lambda_2}{\lambda_1}\frac{\sqrt{\alpha_2}}{\sqrt{\alpha_1}}\left[\frac{e^{\sqrt{\alpha_1}\, x_D} - e^{-\sqrt{\alpha_1}\, x_D}}{2}\right] \tag{65}$$

rearranging equation 63 yields,

$$D = \frac{-\frac{\alpha_3}{\sqrt{\alpha_1}} e^{\sqrt{\alpha_1}\,(x_D - a)}}{e^{\sqrt{\alpha_1}\, x_D}\left[1 - s\frac{\lambda_2}{\lambda_1}\sqrt{\alpha_2} + \frac{\lambda_2}{\lambda_1}\frac{\sqrt{\alpha_2}}{\sqrt{\alpha_1}}\right]} \tag{66}$$

simplifying equation 66 gives the definition of D in the general solution as,

$$D = \frac{-\lambda_1 \alpha_3 e^{-a\sqrt{\alpha_1}}}{\lambda_1\sqrt{\alpha_1} - s\lambda_2\sqrt{\alpha_2}\sqrt{\alpha_1} + \lambda_2\sqrt{\alpha_2}} \tag{67}$$

Substituting equation 67 into equation 57 gives,

$$\bar{p}_{D_1} = \frac{\alpha_3}{\sqrt{\alpha_1}}\left[\frac{e^{\sqrt{\alpha_1}\,(x_D - a)} - e^{-\sqrt{\alpha_1}\,(x_D - a)}}{2}\right]$$

$$- \frac{\lambda_1 \alpha_3 e^{-a\sqrt{\alpha_1}}}{\lambda_1\sqrt{\alpha_1} - s\lambda_2\sqrt{\alpha_2}\sqrt{\alpha_1} + \lambda_2\sqrt{\alpha_2}}$$

$$* \left[\left[1 - s\frac{\lambda_2}{\lambda_1}\sqrt{\alpha_2} \right] \left[\frac{e^{\sqrt{\alpha_1}\, x_D} + e^{-\sqrt{\alpha_1}\, x_D}}{2} \right] \right.$$

$$\left. + \frac{\lambda_2}{\lambda_1}\frac{\sqrt{\alpha_2}}{\sqrt{\alpha_1}} \frac{\left[e^{\sqrt{\alpha_1}\, x_D} - e^{-\sqrt{\alpha_1}\, x_D} \right.}{2} \right] \tag{68}$$

rearranging,

$$\bar{\bar{p}}_{D_1} = \frac{\alpha_3}{2\sqrt{\alpha_1}} \left[e^{\sqrt{\alpha_1}\,(x_D - a)} - e^{-\sqrt{\alpha_1}\,(x_D - a)} \right]$$

$$- \frac{\lambda_1 \alpha_3}{2(\lambda_1\sqrt{\alpha_1} - s\lambda_2\sqrt{\alpha_2}\sqrt{\alpha_1} + \lambda_2\sqrt{\alpha_2})}$$

$$* \left[e^{\sqrt{\alpha_1}\,(x_D - a)} \left[1 - s\frac{\lambda_2}{\lambda_1}\sqrt{\alpha_2} + \frac{\lambda_2}{\lambda_1}\frac{\sqrt{\alpha_2}}{\sqrt{\alpha_1}} \right] \right.$$

$$\left. + e^{-\sqrt{\alpha_1}\,(x_D + a)} \left[1 - s\frac{\lambda_2}{\lambda_1}\sqrt{\alpha_2} - \frac{\lambda_2}{\lambda_1}\frac{\sqrt{\alpha_2}}{\sqrt{\alpha_1}} \right] \right] \tag{69}$$

simplifying,

$$\bar{\bar{p}}_{D_1} = \frac{\alpha_3}{2\sqrt{\alpha_1}} \left[e^{\sqrt{\alpha_1}\,(x_D - a)} - e^{-\sqrt{\alpha_1}\,(x_D - a)} \right] - \frac{\alpha_3}{2\sqrt{\alpha_1}} e^{\sqrt{\alpha_1}\,(x_D - a)}$$

$$- \frac{\alpha_3}{2\sqrt{\alpha_1}}\, e^{-\sqrt{\alpha_1}\,(x_D + a)} \left[\frac{\lambda_1\sqrt{\alpha_1} - s\lambda_2\sqrt{\alpha_2}\sqrt{\alpha_1} - \lambda_2\sqrt{\alpha_2}}{\lambda_1\sqrt{\alpha_1} - s\lambda_2\sqrt{\alpha_2}\sqrt{\alpha_1} + \lambda_2\sqrt{\alpha_2}} \right] \tag{70}$$

yielding for $x_D > a$,

$$\bar{\bar{p}}_{D_1} = - \frac{\alpha_3}{2\sqrt{\alpha_1}} \left[e^{-\sqrt{\alpha_1}\,(x_D - a)} + \left[\frac{\lambda_1\sqrt{\alpha_1} - s\lambda_2\sqrt{\alpha_2}\sqrt{\alpha_1} - \lambda_2\sqrt{\alpha_2}}{\lambda_1\sqrt{\alpha_1} - s\lambda_2\sqrt{\alpha_2}\sqrt{\alpha_1} + \lambda_2\sqrt{\alpha_2}} \right] e^{-\sqrt{\alpha_1}\,(x_D + a)} \right] \tag{71}$$

and for $0< x_D <a$,

$$\bar{\bar{p}}_{D_1} = D\left[1 - s\frac{\lambda_2}{\lambda_1}\sqrt{\alpha_2}\right]\left[\frac{e^{\sqrt{\alpha_1}\,x_D} + e^{-\sqrt{\alpha_1}\,x_D}}{2}\right]$$

$$+ D\frac{\lambda_2}{\lambda_1}\frac{\sqrt{\alpha_2}}{\sqrt{\alpha_1}}\left[\frac{e^{\sqrt{\alpha_1}\,x_D} - e^{-\sqrt{\alpha_1}\,x_D}}{2}\right] \tag{72}$$

substituting D, given by equation 67, into equation 72,

$$\bar{\bar{p}}_{D_1} = \frac{-\lambda_1\alpha_3 e^{-a\sqrt{\alpha_1}}}{\lambda_1\sqrt{\alpha_1} - s\lambda_2\sqrt{\alpha_2}\sqrt{\alpha_1} + \lambda_2\sqrt{\alpha_2}}\left[\left[1 - s\frac{\lambda_2}{\lambda_1}\sqrt{\alpha_2}\right]\left[\frac{e^{\sqrt{\alpha_1}\,x_D} + e^{-\sqrt{\alpha_1}\,x_D}}{2}\right]\right.$$

$$\left. + \frac{\lambda_2}{\lambda_1}\frac{\sqrt{\alpha_2}}{\sqrt{\alpha_1}}\left[\frac{e^{\sqrt{\alpha_1}\,x_D} - e^{-\sqrt{\alpha_1}\,x_D}}{2}\right]\right] \tag{73}$$

rearranging,

$$\bar{\bar{p}}_{D_1} = -\frac{\lambda_1\alpha_3}{2(\lambda_1\sqrt{\alpha_1} - s\lambda_2\sqrt{\alpha_2}\sqrt{\alpha_1} + \lambda_2\sqrt{\alpha_2})}$$

$$* \left[e^{\sqrt{\alpha_1}\,(x_D-a)}\left[1 - s\frac{\lambda_2}{\lambda_1}\sqrt{\alpha_2} + \frac{\lambda_2}{\lambda_1}\frac{\sqrt{\alpha_2}}{\sqrt{\alpha_1}}\right]\right.$$

$$\left. + e^{-\sqrt{\alpha_1}\,(x_D+a)}\left[1 - s\frac{\lambda_2}{\lambda_1}\sqrt{\alpha_2} - \frac{\lambda_2}{\lambda_1}\frac{\sqrt{\alpha_2}}{\sqrt{\alpha_1}}\right]\right] \tag{74}$$

simplifying,

$$\bar{\bar{p}}_{D_1} = -\frac{\alpha_3}{2\sqrt{\alpha_1}}e^{\sqrt{\alpha_1}\,(x_D-a)} - \frac{\alpha_3}{2\sqrt{\alpha_1}}\,e^{-\sqrt{\alpha_1}\,(x_D+a)}$$

$$* \left[\frac{\lambda_1\sqrt{\alpha_1} - s\lambda_2\sqrt{\alpha_2}\sqrt{\alpha_1} - \lambda_2\sqrt{\alpha_2}}{\lambda_1\sqrt{\alpha_1} - s\lambda_2\sqrt{\alpha_2}\sqrt{\alpha_1} + \lambda_2\sqrt{\alpha_2}} \right] \tag{75}$$

giving the solution to $\bar{\bar{p}}_{D_1}$ at $0<x_D<a$ as,

$$\bar{\bar{p}}_{D_1} = -\frac{\alpha_3}{2\sqrt{\alpha_1}} \left[e^{\sqrt{\alpha_1}\,(x_D-a)} \right.$$

$$\left. + \left| \frac{\lambda_1\sqrt{\alpha_1} - s\lambda_2\sqrt{\alpha_2}\sqrt{\alpha_1} - \lambda_2\sqrt{\alpha_2}}{\lambda_1\sqrt{\alpha_1} - s\lambda_2\sqrt{\alpha_2}\sqrt{\alpha_1} + \lambda_2\sqrt{\alpha_2}} \right| e^{-\sqrt{\alpha_1}\,(x_D+a)} \right] \tag{76}$$

Combining equation 71 and 76 by the reciprocity principle for $0<x_D\leq\infty$ gives,

$$\bar{\bar{p}}_{D_1} = -\frac{\alpha_3}{2\sqrt{\alpha_1}} \left[e^{-\sqrt{\alpha_1}\,|x_D-a|} \right.$$

$$\left. + \left[\frac{\lambda_1\sqrt{\alpha_1} - s\lambda_2\sqrt{\alpha_2}\sqrt{\alpha_1} - \lambda_2\sqrt{\alpha_2}}{\lambda_1\sqrt{\alpha_1} - s\lambda_2\sqrt{\alpha_2}\sqrt{\alpha_1} + \lambda_2\sqrt{\alpha_2}} \right] e^{-\sqrt{\alpha_1}\,(x_D+a)} \right] \tag{77}$$

and the solution for $\bar{\bar{p}}_{D_2}$, from equation 43, where $x_D<0$,

$$\bar{\bar{p}}_{D_2} = \frac{-\lambda_1\alpha_3 e^{-a\sqrt{\alpha_1}}}{\lambda_1\sqrt{\alpha_1} - s\lambda_2\sqrt{\alpha_2}\sqrt{\alpha_1} + \lambda_2\sqrt{\alpha_2}} e^{\sqrt{\alpha_2}\,x_D} \tag{78}$$

V. DISCUSSION

Evaluating the analytical solutions, equation 77 and 78, requires inversion through Fourier space and Laplace space back into real space. To accomplish this inversion two programs were developed, the Fourfirst Program which inverts in Fourier space first and the Stehfirst Program which inverts in Laplace space first. (A full discussion of the mechanics of each program is presented in chapter VI.) Comparison of the two programs showed no significant computing advantage of one over the other; if anything, the Stehfirst Program ekecuted approximately 15% faster, in cpu time.

Since the pressure function derived in the analytical solution tends toward oscillation, due to the fourier cosine summation, a convergence criteria was needed to keep check on the values produced from the fourier inversion. The convergence was set to 10^{-14}, meaning that relative changes between summation values needed to change less than 10^{-14} before the value was passed to or from the Laplace inverter. Figure 2 shows the behavior of the inital convergence where $t_D = 0.1$.

After evaluating the soundness of the programs, delimiting parameters were placed on the solution. (See Appendix A for the analytical delimiting solution showing line source concurrence.) The pressure point was situated one wellbore radius away from the well and the vertical no-flow boundary was placed some distance away from the well; equidistant above and below the well. The boundary skin was set to zero, mobility ratios between the two regions were set equally at one as were the diffusivity ratios. Inputting this criteria into the numerical inversions produced the plot shown in figure 3. Figure 3 shows the vertical no-flow boundary, y_D, at 20 with the well located at a = 6, b = 10; the pressure point at $x_D = 7$, $y_D = 10$. No variation between programs was exhibited and as expected, early time data followed strictly along the line source solution.

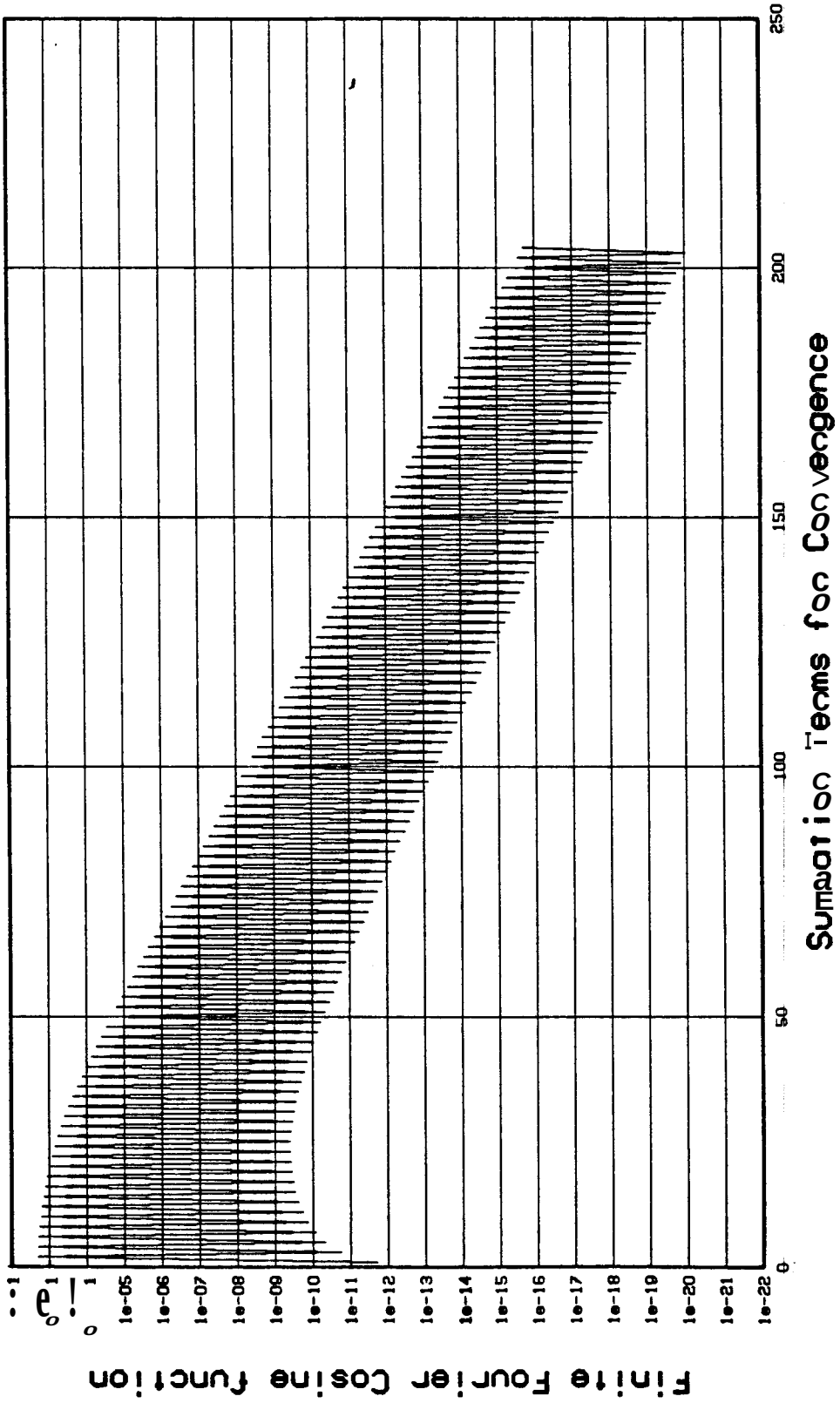

Figure 2 : Semilog plot depicting the behavior of the pressure function during numerical inversion.

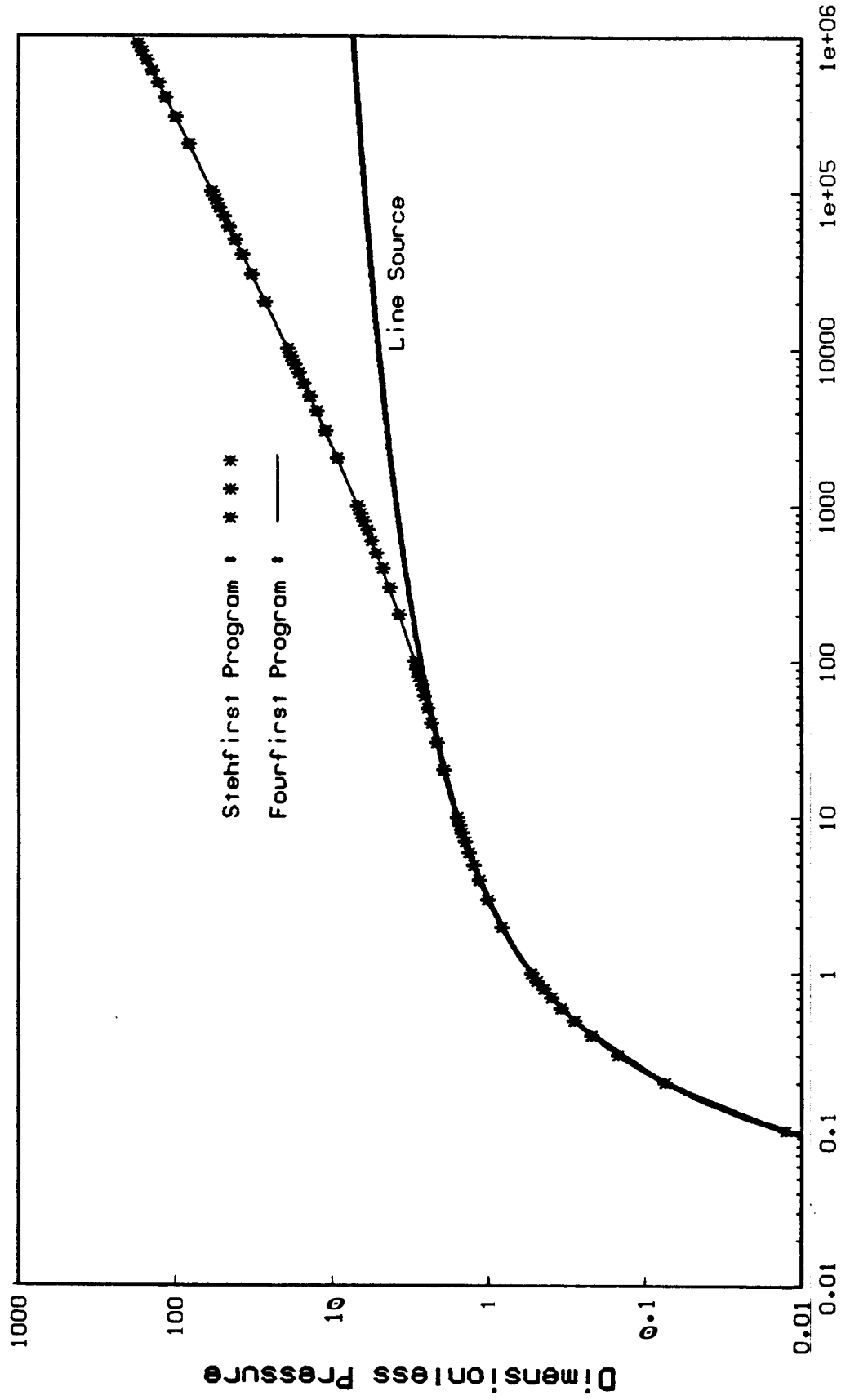

Figure 3 : Logarithmic plot of p_D vs. t_D for values generated at $y^{\circ}_D = 20$ in the Fourfirst and Stehfirst Programs.

Figure 4 is the standard line source solution for varying values of $y°_D$. This array of curves was generated for $10 < y°_D \leq 10000$ using the equation

$$p_D = -\frac{1}{2}\sum_{j=1}^{\infty} Ei\left(-\frac{y°^2_D j^2}{4t_D}\right) - \frac{1}{2} Ei\left(-\frac{1}{4t_D}\right).$$

Using figure 4 for comparison, data was generated using the numerically inverted solution for similar values of $y°_D$. Figure 5 shows these results. As is apparent, no match can be made except for $y°_D = 20$. Using a shifting method the curves were found to follow those in figure 4. Figure 6 shows the shifted results. The shift used was a factor of $y°_D / 20$. The fact that this shift was necessary shows an as yet unresolved puzzle in the analytical solution. This is under further consideration.

Since the data for $y°_D = 20$ shows matching early time data to the line source and half slope behavior at long time, it was used with the line source as a base for the next two cases -- simulation of infinite mobility and infinite skin. To show the behavior of an impermeable boundary *two* alternatives were explored. Figure 7 concerns a high boundary skin, skin=10000. This prohibits communication between region I and II. The late time pressure response doubled that of the open, flowing system. This concurs with the response typically seen with no-flow boundaries such as vertical fractures or sealing faults. This response can similarly be used to evaluate the length to the barrier based on the length of the half slope period. The second case investigated was setting the mobility of fluids in region I infinitely high, $\lambda_1 = 1000$, such that flow with the low mobility fluids of region II was virtually stopped, thus forming a no-flow barrier. Figure 8 shows the anticipated late time half slope curve with double the pressure values of the late time curve with no fluid barrier. (Well location, pressure point location and diffusivities were not changed in either case.)

Appendix C contains selected data for each case discussed herein

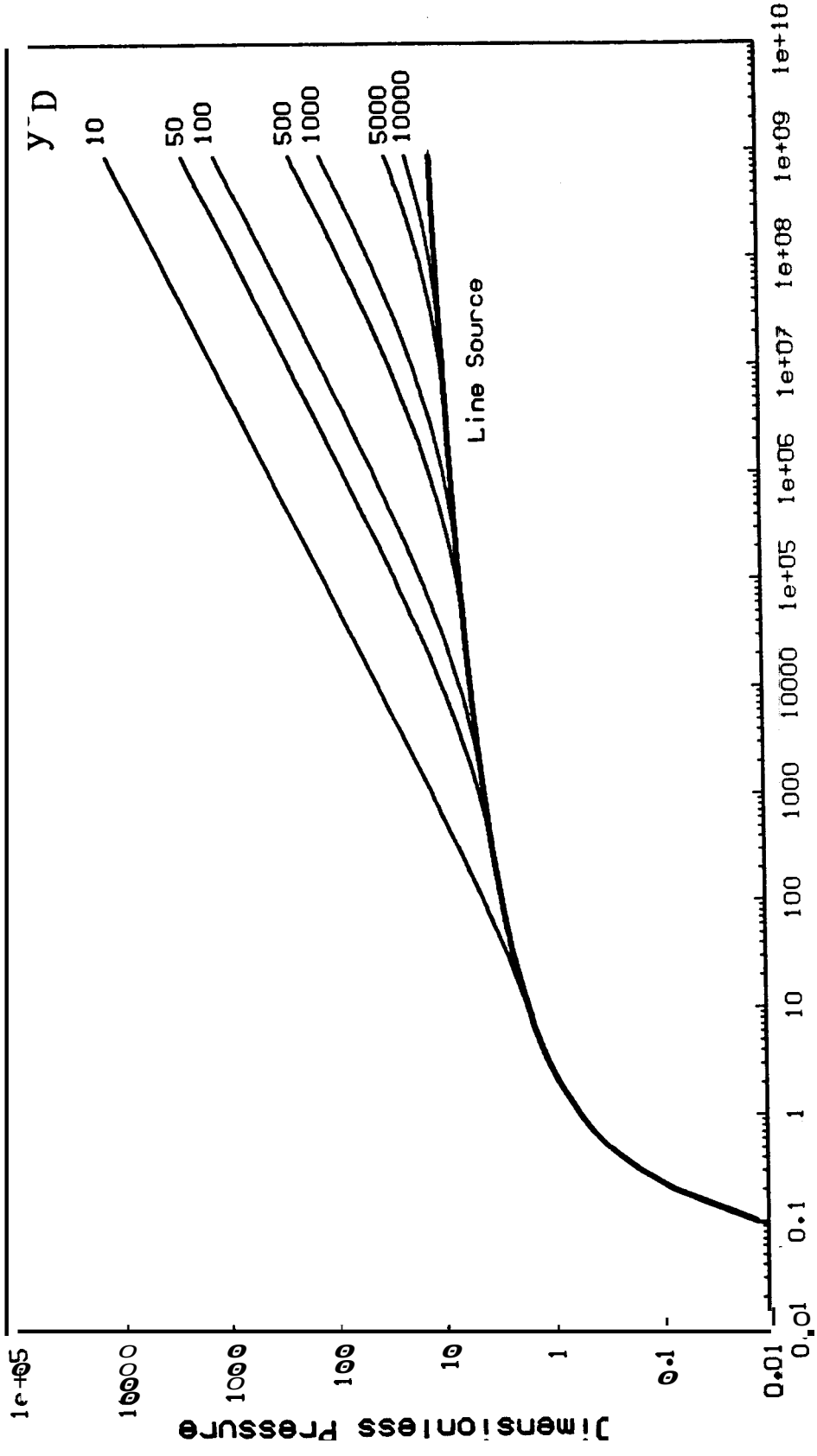

Figure 4 : Logarithmic plot of the sum of line sources with a well located in the center of the system.

$$p_D = -\frac{1}{2}\sum_{j=1}^{\infty} Ei\left(-\frac{y^{\circ 2}_{Dj}}{4t_D}\right) - \frac{1}{2}\,Ei\left(-\frac{1}{4t_D}\right)$$ where y°_D ranges from 10 to 10000.

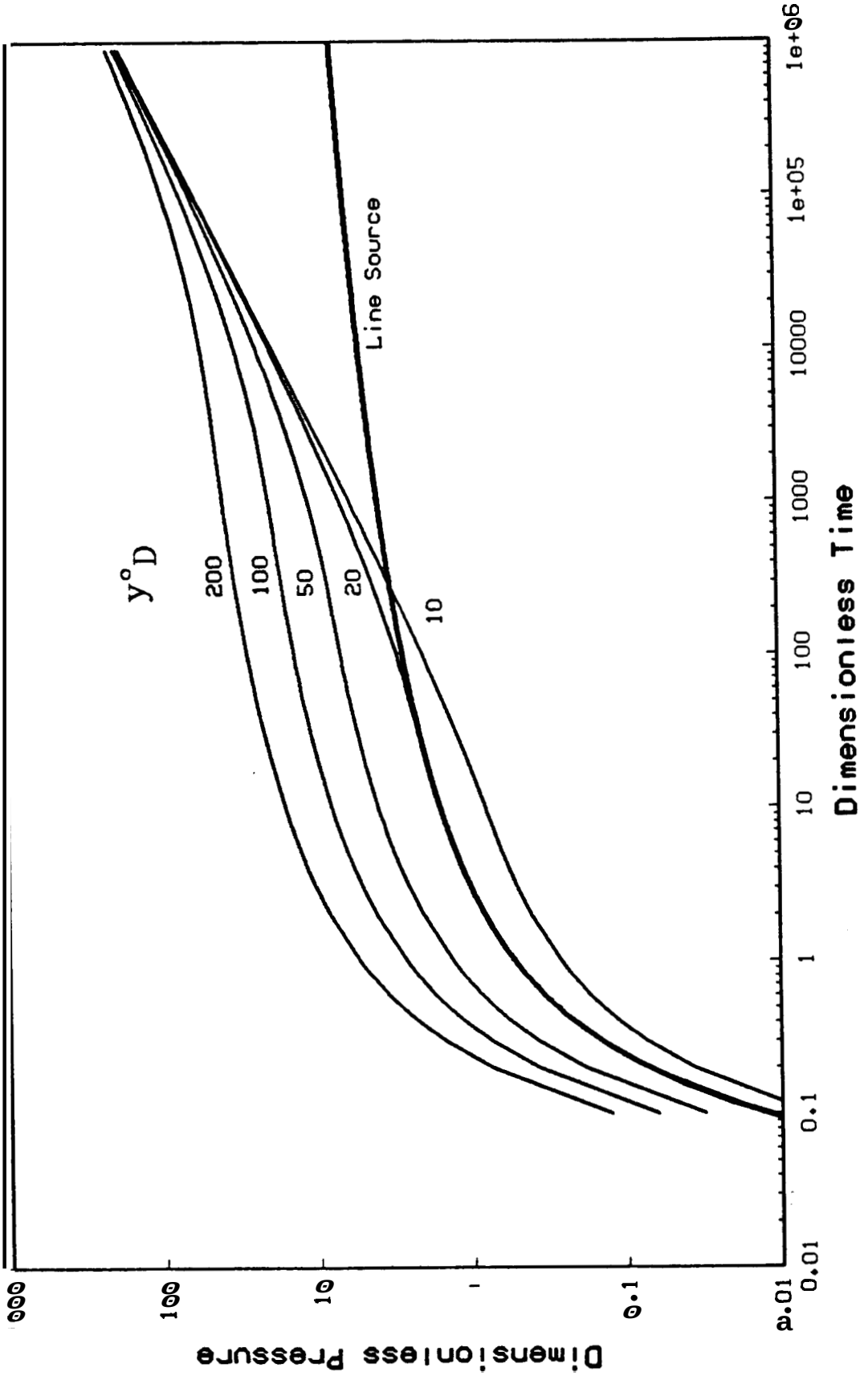

Figure 5 : Logarithmic plot of p_D vs. t_D for composite reservoir with y°_D varying from 10 to 200.

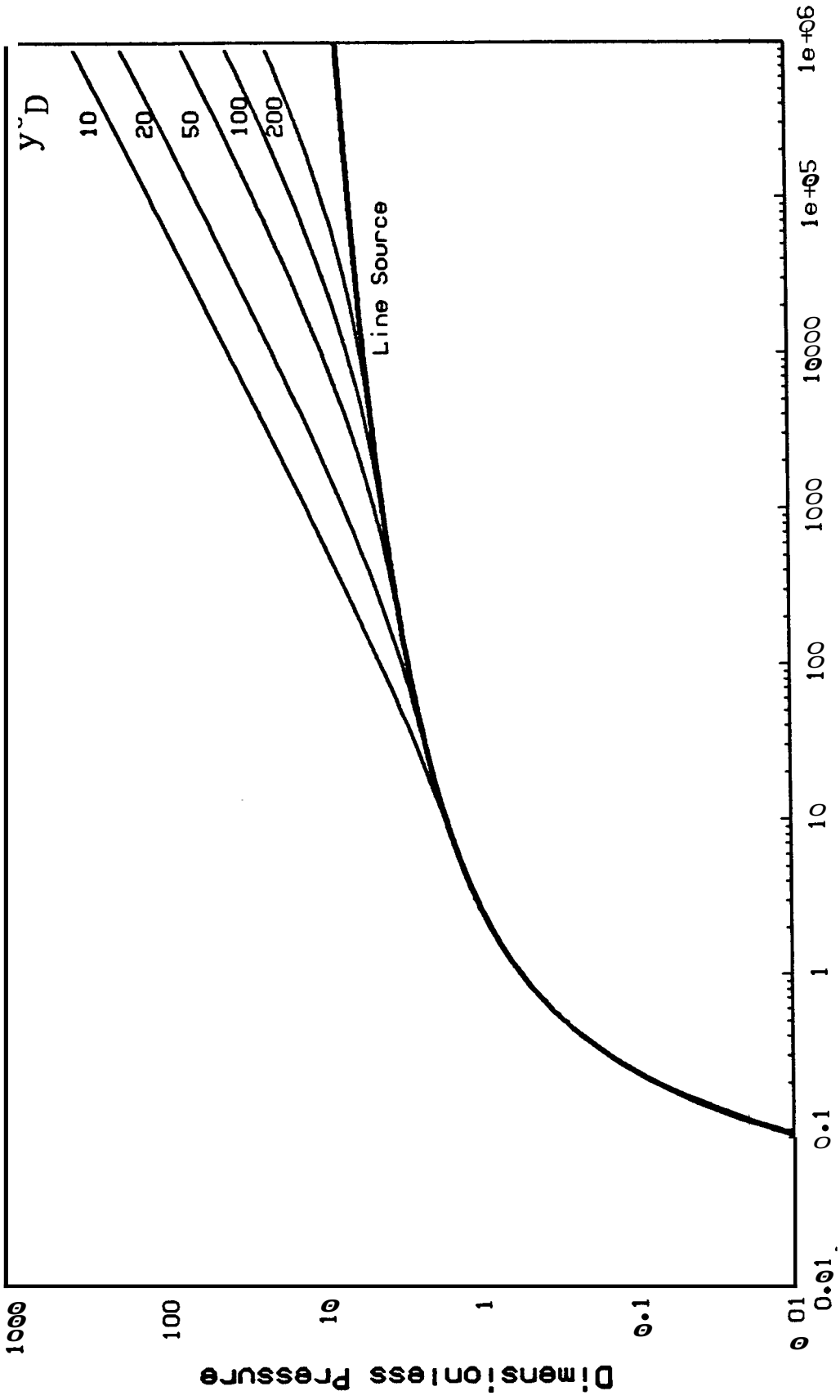

Figure 6 : Logarithmic plot of p_D vs. t_D shifted data from the composite system.

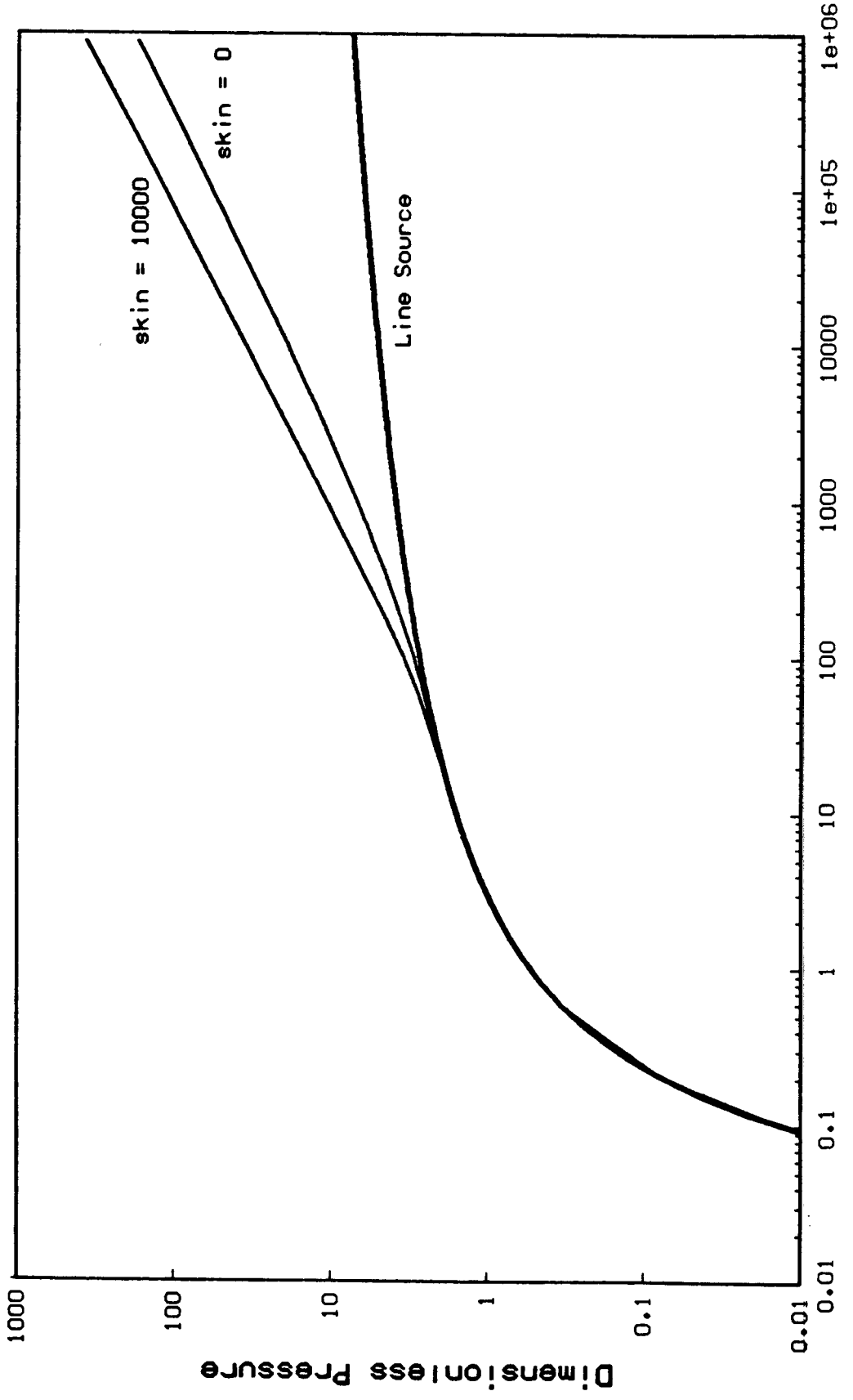

Figure 7 : Logarithmic plot for case of infinite and zero boundary skin.

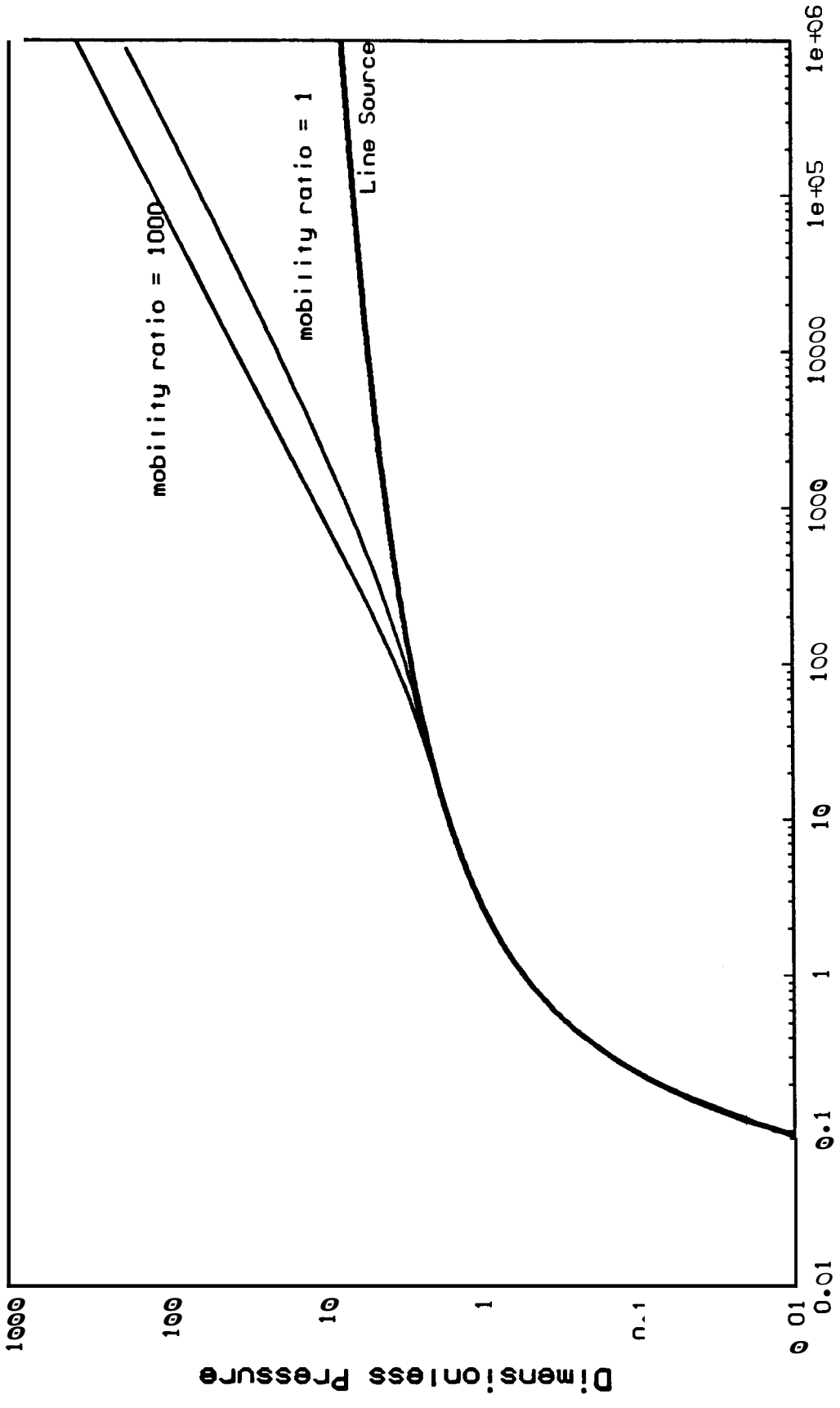

Figure 8 : Logarithmic plot for case of infinite acting unit mobility.

VI. COMPUTATIONAL PROCEDURES

Exact values for the integrals in equations 77 and 78 are evaluated numerically using either of the programs listed in Appendix B. The two programs differ in order of inversion of the problem. The Stehfirst Program inverts the problem in time prior to Fourier inversion of the y variable. The Fourfirst Program, on the other hand, inverts the y variabla prior to the Laplace variable.

Numerical inversion of the governing Laplace equations is facilitated by using an algorithm developed by *Stehfest* [1970]. A fourier inversion algorithm was written to complement the Stehfest algorithm. The fourier inverse transform as defined by *Selby* [1970] is the basis for the algorithm.

The programs are intentionally general such that input data can tailor the problem to be solved. For example, the mobility ratio can be fixed while varying skin in order to observe the pressure effects over time. Additionally, values for pressure are generated on a logorithmic time scale to ease graphing and lessen the accumulation of data once a trend has been established.

Flowcharts for each program are presented in Appendix B preceeding the coding.

VII. CONCLUSIONS AND RECOMMENDATIONS

The objective of this research was to develop a mathematical solution for evaluating transient pressure in a strip reservoir which contains a linear skin discontinuity. An analytical solution was presented with two integral transformations which, due to complexity, were inverted numerically. In evaluating the order of numerical inversion, it was found that using the time inversion prior to space inversion held no advantages over space inversion prior to time inversion.

Verification of results was made by matching the solution to a hypothetical infinite system with the well located centrally and pressure response measured one radii away from the well. It was found for cases of varying vertical no-flow boundaries, the $y°_D$ = 20 case matched; thus leading to a constant shift in data of $y°_D$ / 20 for the accompanying curves. A closer look at the cause of this shift is under consideration. An impermeable boundary was set in two cases by equating mobility ratios to 1000 and, in the second case, by setting the boundary skin to 10000. Late time pressure response concurred doubling of the half slope period as expected.

Future studies using this work as a template can be made studying the effects of varying parameters on the pressure response of the composite infinite strip with a skin boundary.

NOMENCLATURE

a = x coordinate for well location
b = y coordinate for well location
C = constant in the general solution
c = compressibility
D = constant in the general solution
F = Fourier transform operator
h = formation thickness
k = permeability
L = Laplace transform operator
m = Fourier variable
P = pressure
$\bar{p}$ = Laplace transform of p
$\bar{\bar{B}}$ = Fourier transform of $\bar{p}$
$\bar{\bar{p}}$ = Laplace transform of $\bar{p}$
Δp_{skin} = pressure drop across the skin boundary
q = volumetric rate
$q(t)$ = time varying production rate
r = radius
s = dimensionless skin
S = Laplace variable for the time domain
t = time
u = Laplace variable for the x domain
x = x coordinate of the pressure point
Y = y coordinate of the pressure point
y° = finite width of the reservoir
Y = variable transform for y, $\pi y/y^\circ_D$

$\alpha_1 = \nu^2 m^2 + S$
$\alpha_2 = \nu^2 m^2 + \frac{\eta_1}{\eta_2} S$
$\alpha_3 = \frac{\cos(\nu m b)}{S}$
δ = Dirac delta function
η = diffusivity constant
λ = mobility
μ = fluid viscosity
$\nu = \pi/y^\circ_D$
ϕ = formation porosity (fraction)
π = pi, 3.14152976

Subscript

1 = region 1, x>0
2 = region 2, x<0
D = dimensionless
i =initial
t = total system
w = wellbore

REFERENCES

Abramowitz, M., and Stegun, I.A.: ***Handbook of Mathematical Functions,*** Dover Publications, Inc., New York, NY (1970).

Bixel, H.C., Larkin, B.K., and van Poollen, H.K.: "Effects of Linear Discontinuities on Pressure Build-Up and Drawdown Behavior," ***J. Pet. Tech.*** (Aug. 1963) 885-895.

Carslaw, H.S., and Jaeger, J.C.: ***Conduction of Heat in Solids,*** Oxford at the Clarendon Press (1959).

Churchill, R.V.: ***Operational Mathematics,*** McGraw-Hill Book Company (1944).

Cinco, H., Samaniego, F.V., and Dominguez, N.A.: "Unsteady-State Flow Behavior for a Well Near a Natural Fracture," Paper **SPE** 6019 Presented at the 51st Annual Fall Technical Conference and Exhibition of the Society of Petroleum Engineers of AIME, New Orleans, LA (Oct. 1976).

Collins, R.E.: ***Flow of Fluids Through Porous Materials,*** Reinhold Publishing Corp., New York, ***NY*** (1961).

Davis, G.E., and Hawkins, M.F.: "Linear Fluid-Barrier Detection by Well Pressure Measurements," ***J. Per. Tech.*** (Oct. 1963) 1077-1079.

Earlougher, R.C., Ramey, H.J., Jr., Miller, F.G., and Mueller, T.D.: "Pressure Distribution in Rectangular Reservoirs," ***J.*** Pet. ***Tech.*** (Feb. 1968) 199-208.

Elkins, L.F., and Skov, A.M.: "Anisotropic Spread of Pressure Transients Delineates Sprabeny Fracture Orientation," Trans., AIME (1960) ***219***, 301.

Fenske, P.R.: "Unsteady Drawdown in the Presence of ***a*** Linear Discontinuity," ***Groundwater Hydraulics,*** Water Resources Monograph 9 (1984).

Gibson, J.A., and Campbell, A.T.: "Calculating the Distance to a Discontinuity from D.S.T. Data," Paper **SPE** 3016 Presented at the **45th** Annual Fall Meeting of the Society of Petroleum Engineers of AIME, Houston, TX (Oct. 1970).

Hildebrand, F.B.: ***Advanced Calculus for Applications,*** Prentice-Hall, Inc., Englewood Cliffs, N.J. (1976).

Homer, D.R.: "Pressure Build-Up in Wells," ***Reprint Series, No. 9 - Pressure Analysis Methods,*** Society of Petroleum Engineers of AIME, Dallas, TX (1967) 25-43.

Hurst, W.: "Interference Between Oil Fields," ***Trans.,*** AIME (1960) ***219,*** 175-192.

Kaplan, **W.** : ***Advanced Mathematics for Engineers,*** Addison-Wesley Publishing Company (1981).

Matthews, C.S., Brons, **F.,** and Hazebroek, P.: "A Method for Determination of Average Pressure in a Bounded Reservoir," ***Trans.,*** AIME (1954) ***201,*** 182-191.

Matthews, C.S., and Russell, D.C.: ***Pressure Buildup and Flow Tests in Wells,*** Monograph Series, Society of Petroleum Engineers of AIME, Dallas, TX **(1967).**

Muskat, M.: ***The Flow of Homogeneous Fluids Through Porous Media,*** IHRDC, Publishers, Boston, MA **(1937).**

Prasad, R.K.: **"Pressure** Transient Analysis in the Presence of Two Intersecting Boundaries," ***Trans.,*** AIME **(1975)** *259,* **89.**

Ramey, H.J., Jr., **Kumar,** A. and Gulati, M.S.: **Gar** ***Well Test Analysis Under Water Drive Conditions,*** American **Gas** Association, Arlington, VA **(1973).**

Sageev A., Home R. N., Ramey H. J., Jr.: "Detection of Linear Boundaries by Drawdown Tests: A Semilog Curve Matching Approach," ***Water Resources Research. vol. 21, no.3,*** **305-310.**

Selby, S.M.: ***Standard Mathematical Tables,*** **18th** Edition, The Chemical Rubber Company, Cleveland, OH **(1970).**

Stallman, R.W.: "Nonequilibrium Type Curves Modified for Two-Well Systems," ***US Geol. Sun.,*** Groundwater Note **3 (1952).**

Standing, M.B.: "Linear Fluid-Barrier Detection by Well Pressure Measurements," -Discussion, ***J. Pet. Tech.,*** **(Mar. 1964) 259-260.**

Stehfest, **H.:**"Algorithm **368,** Numerical Inversion of Laplace Transforms," ***Communications of the ACM, D-5*** (Jan. **1970) 13,** No.1, **47-49.**

Tiab, D., and Kumar, A.: "Detection and Location of Two Parallel Sealing Faults Around a Well," ***J. Pet. Tech.*** **(Oct. 1980) 1701-1708.**

Van Everdingen, A.F., and Hurst, **W.:**"The Application of the Laplace Transformation to Flow Problems in Reservoirs," Trans., AIME **(1949) 286, 305-324.**

Yaxley, **L.M.:** "The Effect of a Partially Communicating Fault on Transient Pressure Behavior," Paper **SPE 14311** Presented at the **60th Annual** Fall meeting of the Society of Petroleum Engineers of AIME, Las Vegas, NV (Sept. **1985).**

APPENDIX A : Delimiting Solution For Line Source Concurrence

Delimiting Solution for Line Source Concurrence

In evaluating the validity of the derived solutions, a reduction of the Solution can be made such that a comparison with the line source solution is posssible. Assuming the conditions the line source was developed under will be repeated for equation 71 where $x_D > a$.

Isolating equation 71,

$$\bar{\bar{p}}_{D_1} = -\frac{\alpha_3}{2\sqrt{\alpha_1}}\left[e^{-\sqrt{\alpha_1}(x_D-a)} + \left[\frac{\lambda_1\sqrt{\alpha_1} - s\lambda_2\sqrt{\alpha_2}\sqrt{\alpha_1} - \lambda_2\sqrt{\alpha_2}}{\lambda_1\sqrt{\alpha_1} - s\lambda_2\sqrt{\alpha_2}\sqrt{\alpha_1} + \lambda_2\sqrt{\alpha_2}}\right]e^{-\sqrt{\alpha_1}(x_D+a)}\right]$$

letting α_1, α_2, and α_3 revert to their substituting parameters and assuming the following:

$$x_D - a = 1 \tag{79}$$

$$s = 0 \tag{80}$$

$$\lambda_1/\lambda_2 = \eta_1/\eta_2 = 1 \tag{81}$$

equation 71 reduces to

$$\bar{\bar{p}}_{D_1} = -\frac{e^{-\sqrt{v^2m^2+S}}\cos(vmb)}{2S\sqrt{v^2m^2+S}} \tag{82}$$

Recalling the Finite Fourier Cosine Inverse Transformation from *Selby* [1970] defined for $0 < Y_D < \pi$,

$$\bar{F}(Y) = \frac{1}{\pi}f_c(0) - \frac{2}{\pi}\sum_{m=1}^{\infty} f_c(m)\cos(mY_D) \tag{83}$$

where Y_D will be defined in the center of the system at $Y_D = \pi/2$.

Applying equation 83 to equation 82 gives,

$$\bar{p}_{D_1} = -\frac{e^{-\sqrt{S}}}{2\pi S\sqrt{S}} - \frac{2}{\pi}\sum_{m=\text{even}}^{\infty}\frac{e^{-\sqrt{v^2m^2+S}}}{S\sqrt{v^2m^2+S}}\frac{\cos(vmb)\cos(mY_D)}{2} \tag{84}$$

letting

$$w = \nu m \tag{85}$$

equation 84 becomes:

$$\bar{p}_{D_1} = -\frac{e^{-\sqrt{S}}}{2\pi S\sqrt{S}} - \frac{2}{\pi}\sum_{m=even}^{\infty}\frac{e^{-\sqrt{w+S}}}{S\sqrt{w+S}}\,\frac{cos(wb)\ cos(mY_D)}{2} \tag{86}$$

Recalling the following Laplace inverse transformations from *Churchill* [1944]:

$$L^{-1}\left[S^{-3/2}e^{-\sqrt{S}}\right] = 2\sqrt{\frac{t}{\pi}}\,e^{-\frac{1}{4t}} - erfc\left(\frac{1}{2\sqrt{t}}\right) \tag{87}$$

$$L^{-1}\left[\frac{e^{-w_1\sqrt{S}}}{\sqrt{S}}\right] = \frac{1}{\sqrt{\pi t}}\,e^{-\frac{w_1^2}{4t}} = F(t) \tag{88}$$

and

$$L^{-1}\left[-\frac{\cos(wb)\ cos(mY_D)}{2S}\right] = -\frac{\cos(wb)\ cos(mY_D)}{2} \tag{89}$$

letting $w_1 = 1$ and applying the following substitution,

$$f(S+w^2) = \int_0^{\infty} e^{-w^2 t}\,F(t)\,e^{-St}\,dt \tag{90}$$

such that equation (88) takes the form,

$$L^{-1}\left[\frac{e^{-w_1\sqrt{w^2+S}}}{\sqrt{w^2+S}}\right] = e^{-w^2 t}\left(\frac{e^{-\frac{1}{4t}}}{\sqrt{\pi t}}\right) \tag{91}$$

then, in real space and time, equation 86 becomes:

$$p_{D_1} = -\frac{1}{2\pi}\left[2\sqrt{\frac{t_D}{\pi}}\,e^{-\frac{1}{4t_D}} - erfc\left(\frac{1}{2\sqrt{t_D}}\right)\right]$$
$$-\frac{2}{\pi}\sum_{m=even}^{\infty} -\frac{\cos(wb)\cos(mY_D)}{2\sqrt{\pi}} * \int_0^{t_D} \frac{e^{-w^2\tau - \frac{1}{4\tau_D}}}{\sqrt{\tau}}\,d\tau \qquad (92)$$

Evaluation of the integral in equation 92 is facilitated by use of the following substitutions from *Abramowitz and Stegun* [1970]:

let

$$\omega = w \qquad (93)$$

$$\beta = \frac{1}{2} \qquad (94)$$

$$\chi^2 = \tau \qquad (95)$$

and

$$d\tau = 2\chi d\chi \qquad (96)$$

applying these substitutions to the following integral defined in *Abramowitz and Stegun* [1970] yields,

$$\int e^{-\omega^2\chi^2 - \frac{\beta^2}{\chi^2}}\,d\chi = \frac{\sqrt{\pi}}{4\omega}\left[e^{2\omega\beta}\,erf\left(\omega\chi + \frac{\beta}{\chi}\right)\right.$$
$$\left. + e^{-2\omega\beta}\,erf\left(\omega\chi - \frac{\beta}{\chi}\right)\right] + constant \qquad (97)$$

Equation 97 can be directly applied to the integral in equation 92 and evaluated at the limits of 0 to t_D:

$$2\int_0^{t_D} e^{-\omega^2\chi^2-\frac{\beta^2}{\chi^2}}\,d\chi = \frac{2\sqrt{\pi}}{4\omega}\left[e^{2\omega\beta}\,erf(\omega t_D+\frac{\beta}{t_D}) + e^{-2\omega\beta}\,erf(\omega t_D-\frac{\beta}{t_D})\right] \tag{98}$$

Reverting the substitution of w for ω and 1/2 for β gives,

$$\int_0^{t_D} \frac{e^{-w^2\tau-\frac{1}{4\tau_D}}}{\sqrt{\tau}}\,d\tau = \frac{\sqrt{\pi}}{2w}\left[e^{w}\,erf(wt_D+\frac{1}{2t_D}) + e^{-w}\,erf(wt_D-\frac{1}{2t_D})\right] \tag{99}$$

Rearranging equation 99 and substituting νm back for w gives the following solution:

$$p_{D_1} = -\frac{1}{2\pi}\left[2\sqrt{\frac{t_D}{\pi}}\,e^{-\frac{1}{4t_D}} - erfc(\frac{1}{2\sqrt{t_D}})\right]\frac{1}{2\pi} *$$

$$* \sum_{m=even}^{\infty} \frac{1}{\nu m}\left[e^{\nu m}\,erf(\nu m t_D+\frac{1}{2t_D}) + e^{-\nu m}\,erf(\nu m t_D-\frac{1}{2t_D})\right] \tag{100}$$

APPENDIX B : Computer Programs

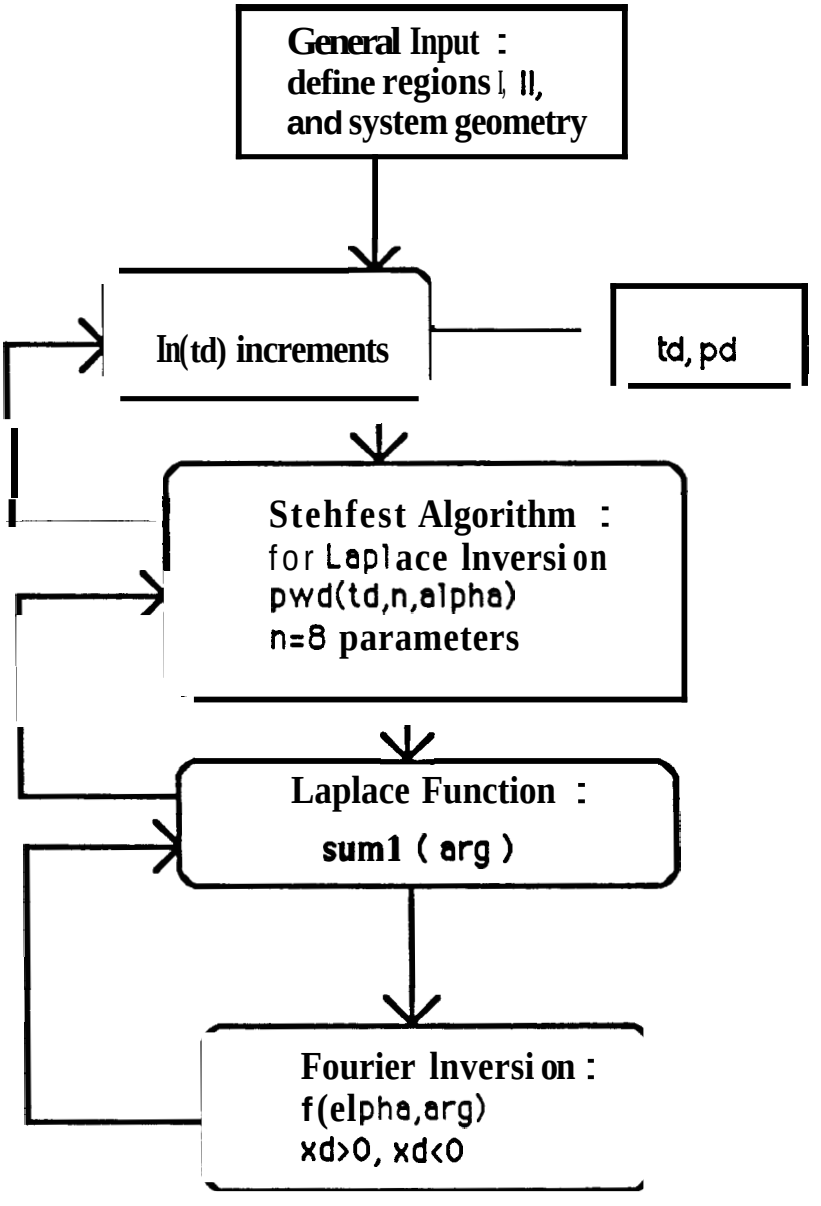

Figure 9 : Flowchart for Fourfirst Program

```
C                    PROGRAM FOURFIRST
C
C
C
C
C     This program generates pd versus td for a system containing a
C        linear skin discontinuity.  Numerical inversion of pd is
C        accomplished by first inverting the Fourier function in the
C        y domain then inverting the Laplace function in time.
C
C     Variable Definitions:
C
C              n = number of parameters for the Stehfest Algorithm
C              m = calculation flag
C             td = dimensionless time
C            pdw = dimensionless pressure
C            pwd = function called within Stehfest that contains Laplace
C                  equation to be inverted
C           pwdl = Stehfest function that inverts Laplace equation
C           sum1 = function called within Fourier Inverter containg the
C                  Finite Fourier Cosine equation to be inverted
C              f = Fourier function that inverts the Finite Fourier Cosine
C                  equation
C            arg = Laplace variable
C          alpha = Fourier variable
C             xd = dimensionless x coordinate defining the pressure point
C             yd = dimensionless y coordinate defining the pressure point
C              a = dimensionless x coordinate defining the well location
C              b = dimensionless y coordinate defining the well location1
C
C
C      Input required by the program is read in from a file called
C         'data.in'.  Contents of the data file are the well and pressure
c         locations, skin, dimension of the system in the y direction, and
C         formation properties.
C      Output appears in a file called 'data.out' which contains the values
C          for pd vs. td.


      implicit real*8(a-h,o-z)
      real*8 nu,i,k,l,mm,nn
      common a,b,yod,skin,xd,yd,eta1,eta2,alam1,alam2,m

      open(unit=3, file='data.out')
      rewind(unit=3)
      open(unit=4, file='damin', status='old', access='sequential')
      rewind(unit=4)

      read(4,*)a,b,yod,skin,xd,yd,eta1,eta2,alam1,alam2
      write(3,7)a,b,yod,skin,xd,yd,eta1,eta2,alam1,alam2
7     format(5x,'data: a= ',f3.1,1x,'b= ',f4.1,1x,'yod= ',f6.1,1x,
     +'skin= ',f3.1,1x,'xd= ',f3.1,1x,'yd= ',f4.1,/,12x,'eta1= ',
     +f3.1,1x,'eta2= ',f3.1,1x,'alam1= ',f3.1,1x,'alam2= ',f3.1)
```

```
      pi=3.14152976
      nu=pi/yod

      m=777
      n=8
      do 10 i=0,6
           k=10**i
           l=k*10
           mm=2*k

        do 20 nn=mm,l,k
             td=nn

             call pwd(td,n,pdw)
             write(3,*)td,pdw

20         continue
10       continue

      stop
      end
```

```
C              THE STEHFEST ALGORITHM
C             ****************************
C
      SUBROUTINE PWD(TD,N,PD)
C          THIS FUNTION COMPUTES NUMERICALLY THE LAPLACE TRNSFORM
C          INVERSE OF F(S).
      IMPLICIT  REAL*8 (A-H,O-Z)
      DIMENSION G(50),V(50),H(25)
      common a,b,yod,skin,xd,yd,eta1,eta2,alam1,alam2,m
C
C          NOW IF THE ARRAY V(I) WAS COMPUTED BEFORE THE PROGRAM
C          GOES DIRECTLY TO THE END OF THE SUBRUTINE TO CALCULATE
C          F(S).
      IF (N.EQ.M) GO TO 17
      M=N
      DLOGTW=0.6931471805599
      NH=N/2
C
C          THE FACTORIALS OF 1 TO N ARE CALCULATED INTO ARRAY G.
      G(1)=1
      DO 1 I=2,N
        G(I)=G(I-1)*I
1     CONTINUE
C
C          TERMS WITH K ONLY ARE CALCULATED INTO ARRAY H.
      H(1)=2./G(NH-1)
      DO 6 I=2,NH
```

```
      FI=I
      IF(I-NH) 4,5,6
4     H(I)=FI**NH*G(2*I)/(G(NH-I)*G(I)*G(I-1))
      GO TO 6
5     H(I)=FI**NH*G(2*I)/(G(I)*G(I-1))
6   CONTINUE
C
C       THE TERMS (-1)**NH+1 ARE CALCULATED.
C       FIRST THE TERM FOR 1=1
    SN=2*(NH-NH/2*2)-1
C
C       THE REST OF THE SN'S ARECALCULATED IN THE MAIN RUTINE.
C
C
C       THE ARRAY V(I) IS CALCULATED.
    DO 7 I=1,N
C
C       FIRST SET V(I)=0
      V(I)=0.
C
C       THE LIMITS FOR K ARE ESTABLISHED.
C       THE LOWER LIMIT IS K1=INTEG((I+1/2))
      K1=(I+1)/2
C
C       THE UPPER LIMIT IS K2=MIN(I,N/2)
      K2=I
      IF (K2-NH) 8,8,9
9     K2=NH
C
C       THE SUMMATION TERM IN V(I) IS CALCULATED.
8     DO 10 K=K1,K2
        IF (2*K-I) 12,13,12
12       IF (I-K) 11,14,11
11       V(I)=V(I)+H(K)/(G(I-K)*G(2*K-I))
        GOTO 10
13       V(I)=V(I)+H(K)/G(I-K)
        GOTO 10
14       V(I)=V(I)+H(K)/G(2*K-I)
10     CONTINUE
C
C       THE V(I) ARRAY IS FINALLY CALCULATED BY WEIGHTING
C       ACCORDING TO SN.
      V(I)=SN*V(I)
C
C       THE TERM SN CHANGES ITS SIGN EACH ITERATION.
      SN=-SN
7   CONTINUE
C
C       THE NUMERICAL APPROXIMATION IS CALCULATED.
17  PD=0.0
    PMCA=DLOGTW/TD
    DO 15 I=1,N
      ARG=PMCA*I
      funs=sum1(arg)
```

```
      PD=PD+V(I)*funs
15    CONTINUE
      PD=PD*PMCA
18    RETURN
      END
```

```
      function sum1(arg)
      implicit real*8(a-h,o-z)
      real*8 nu
      common a,b,yod,skin,xd,yd,eta1,eta2,alam1,alam2,m

      pi=3.14152976
      nu=pi/yod
      yyd=pi*yd/yod
      argo=0.0
      fun1=f(arg0,arg)
      sumo=fun1
      sum=sum0
      sum2=10
      sum3=10

c     starting the computation loop
        do 20 j=1,5000
          arg2=j
          fun2=f(arg2,arg)
          sum5=fun2*cos(j*yyd)
          sum4=sum2
          sum2=sum3
          sum3=sum5
          sum=sum+sum5
          adelta=(abs(sum3)+abs(sum2)+abs(sum4))/sum
          delta=abs(adelta)
          if(delta.lt.0.00000000000001) goto 999
20        continue

999       sum1=-((1.0/pi)*fun1+(2.0/pi)*(sum-fun1))

      return
      end
```

```
      double precision function f(alpha,arg)
      implicit real*8 (a-h,o-z)
      real*8 nu
      common a,b,yod,skin,xd,yd,eta1,eta2,alam1,alam2,m
```

```
      pi=3.14152976
      nu=pi/yod

      f1=sqrt(nu*nu*alpha*alpha+arg)
      f2=sqrt(nu*nu*alpha*alpha+eta1/eta2*arg)
      f3=alam1*f1-skin*alam2*f2*f1+alam2*f2
      f4=alam1*f1-skin*alam2*f2*f1-alam2*f2

      if(xd.gt.0.0) then
      f=(-cos(nu*alpha*b)/(2.0*arg*f1))*(dexp(-f1*abs(xd-a))
     *+f4/f3*dexp(-f1*(xd+a)))
      else
      f=(-alam1*cos(nu*alpha*b)*dexp(f2*xd-a*f1))/(arg*f3)
      endif

      return
      end
```

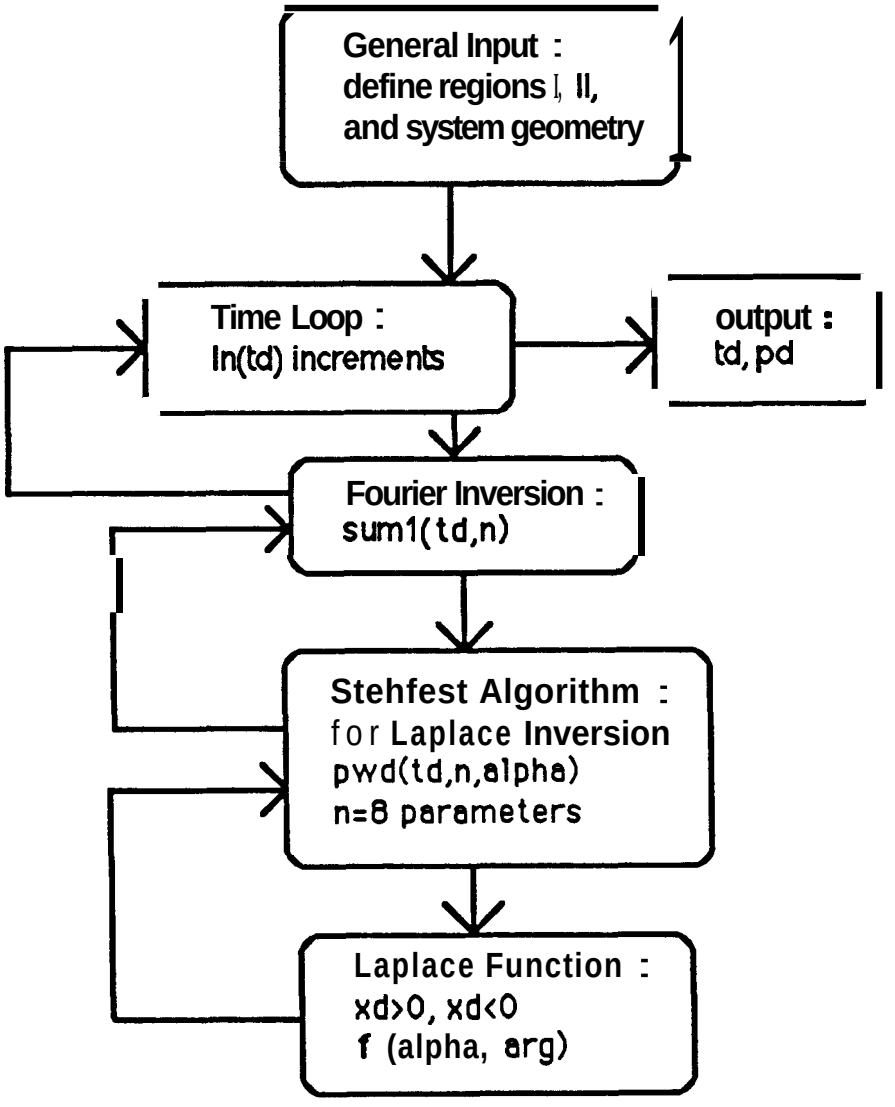

Figure 10 : Flowchart for Stehfirst Program

```
C                    PROGRAM STEHFIRST
C
C
C
C     This program generates pd versus td for a system containing a
C          linear skin discontinuity.  Numerical inversion of pd is
C          accomplished by first inverting the Laplace function in
C          time then inverting the Finite Fourier function in the y
C          domain.
C
C     Variable Definitions:
C
C               n = number of parameters for the Stehfest Algorithm
C               m = calculation flag
C              td = dimensionless time
C              pd = dimensionless pressure
C             pwd = function called within Stehfest that contains Laplace
C                   equation to be inverted
C            pwdl = Stehfest function that inverts Laplace equation
C            sum1 = function called within Fourier Inverter containing the
C                   Finite Fourier Cosine equation to be inverted
C               f = Fourier function that inverts the Finite Fourier Cosine
C                   equation
C             arg = Laplace variable
C           alpha = Fourier variable
C              xd = dimensionless x coordinate defining the pressure point
C              yd = dimensionless y coordinate defining the pressure point
C               a = dimensionless x coodinate defining the well location
C               b = dimensionless y coordinate defining the well location
C
C
C      Input required by the program is read in from a file called
C           'data.in'.  Contents of the data file are the well and pressure
C           locations, skin, dimension of the system in the y direction, and
C           formation properties.
C      Output appears in a file called 'data.out' which contains the values
C           for pd vs. td.


      implicit real*8(a-h,o-z)
      real*8 nu,i,k,l,mm,nn
      common a,b,yod,skin,xd,yd,eta1,eta2,alam1,alam2,m

      open(unit=3, file='data.out')
      rewind(unit=3)
      open(unit=4, file='data.in', status='old', access='sequential')
      rewind(unit=4)

      read(4,*)a,b,yod,skin,xd,yd,eta1,eta2,alam1,alam2
      write(3,7)a,b,yod,skin,xd,yd,eta1,eta2,alam1,alam2
7     format(5x,'data: a= ',f3.1,1x,'b= ',f4.1,1x,'yod= ',f6.1,1x,
     +'skin= ',f3.1,1x,'xd= ',f3.1,1x,'yd= ',f4.1,/,12x,'eta1= ',
     +f3.1,1x,'eta2= ',f3.1,1x,'alam1= ',f3.1,1x,'alam2= ',f3.1)
```

```
      pi=3.14152976
      nu=pi/yod

      m=777
      n=8
      do 10 i=0,6
            k=10**i
            l=k*10
            mm=2*k

         do 20 nn=mm,l,k
               td=nn

               pd=sum1(td,n)
               write(3,*)td,pd
               print *, td,pd

20          continue
10       continue

      stop
      end




      function sum1(td,n)
      implicit real*8(a-h,o-z)
      real*8 nu
      common a,b,yod,skin,xd,yd,eta1,eta2,alam1,alam2,m

      pi=3.14152976
      nu=pi/yod
      yyd=pi*yd/yod
      arg0=0.0
      fun1=pwd(td,n,arg0)
      sum=fun1
      sum2=10
      sum3=10

c     starting the computation loop
        do 20 j=1,5000
          arg2=j
          fun2=pwd(td,n,arg2)
          sum5=fun2*cos(j*yyd)
          sum4=sum2
          sum2=sum3
          sum3=sum5
          sum=sum+sum5
          adelta=(abs(sum3)+abs(sum2)+abs(sum2))/sum
          delta=abs(adelta)
          if(delta.lt.0.00000000000001) goto 999
```

```
20      continue

999     sum1=-((1.0/pi)*fun1+(2.0/pi)*(sum-fun1))

        return
        end
```

```
C            THE STEHFEST ALGORITHM
C          ****************************
C
      FUNCTION PWD(TD,N,ALPHA)
C       THIS FUNTION COMPUTES NUMERICALLY THE LAPLACE TRNSFORM
C       INVERSE OF F(S).
      IMPLICIT  REAL*8 (A-H,O-Z)
      DIMENSION G(50),V(50),H(25)
      common a,b,yod,skin,xd,yd,eta1,eta2,alam1,alam2,m
C
C       NOW IF THE ARRAY V(I) WAS COMPUTED BEFORE THE PROGRAM
C       GOES DIRECTLY TO THE END OF THE SUBRUTINE TO CALCULATE
C       F(S).
      IF (N.EQ.M) GO TO 17
      M=N
      DLOGTW=0.693147 1805599
      NH=N/2
C
C       THE FACTORIALS OF 1 TO N ARE CALCULATED INTO ARRAY G.
      G(1)=1
      DO 1 I=2,N
        G(I)=G(I-1)*I
    1  CONTINUE
C
C       TERMS WITH K ONLY ARE CALCULATED INTO ARRAY H.
      H(1)=2./G(NH-1)
      DO 6 I=2,NH
        FI=I
        IF(I-NH) 4,5,6
    4   H(I)=FI**NH*G(2*I)/(G(NH-I)*G(I)*G(I-1))
        GO TO 6
    5   H(I)=FI**NH*G(2*I)/(G(I)*G(I-1))
    6  CONTINUE
C
C       THE TERMS (-1)**NH+1 ARE CALCULATED.
C       FIRST THE TERM FOR I=1
      SN=2*(NH-NH/2*2)-1
C
```

```
C       THE REST OF THE SN'S ARECALCULATED IN THE MAIN RUTINE.
C
C
C       THE ARRAY V(I) IS CALCULATED.
      DO 7 I-l,N
C
C       FIRST SET V(I)=0
        V(I)=0.
C
C       THE LIMITS FOR K ARE ESTABLISHED.
C       THE LOWER LIMIT IS K1=INTEG((I+1/2))
        K1=(I+1)/2
C
C       THE UPPER LIMIT IS K2=MIN(I,N/2)
        K2=I
        IF (K2-NH) 8,8,9
9       K2-NH
C
C       THE SUMMATION TERM IN V(I) IS CALCULATED.
8       DO 10 K=K1,K2
          IF (2*K-I) 12,13,12
12         IF (I-K) 11,14,11
11         V(I)=V(I)+H(K)/(G(I-K)*G(2*K-I))
          GOTO 10
13         V(I)=V(I)+H(K)/G(I-K)
          GOTO 10
14         V(I)=V(I)+H(K)/G(2*K-I)
10       CONTINUE
C
C       THE V(I) ARRAY IS FINALLY CALCULATED BY WEIGHTING
C       ACCORDING TO SN.
        V(I)=SN*V(I)
C
C       THE TERM SN CHANGES ITS SIGN EACH ITERATION.
        SN=-SN
7     CONTINUE
C
C       THE NUMERICAL APPROXIMATION IS CALCULATED.
17    PWD=0.0
      PMCA=DLOGTW/TD
      DO 15 I=1,N
        ARG=PMCA*I
        funs=f(alpha,arg)
        PWD=PWD+V(I)*funs
15    CONTINUE
      PWD=PWD*PMCA
18    RETURN
      END
```

```
      function f(alpha,arg)
      implicit real*8 (a-h,o-z)
      real*8 nu
      common a,b,yod,skin,xd,yd,eta1,eta2,alam1,alam2,m

      pi=3.14152976
      nu=pi/yod

      f1=sqrt(nu*nu*alpha*alpha+arg)
      f2=sqrt(nu*nu*alpha*alpha+eta1/eta2*arg)
      f3=alam1*f1-skin*alam2*f2*f1+alam2*f2
      f4=alam1*f1-skin*alam2*f2*f1-alam2*f2

      if(xd.gt.0.0) then
      f=(-cos(nu*alpha*b)/(2.0*arg*f1))*(dexp(-f1*abs(xd-a))
     *+f4/f3*dexp(-f1*(xd+a)))
      else
      f=(-alam1*cos(nu*alpha*b)*dexp(f2*xd-a*f1))/(arg*f3)
      endif

      return
      end
```

APPENDIX C : Selected Data

TABLE C-1

Selected Data from Stehfirst and Fourfirst Program Evaluation

Stehfirst Program :

$y^{\circ}_D = 20$
skin = 0
a = 6
b = 10
$x_D = 7$
$y_D = 10$
$\lambda_1 = \lambda_2 = \eta_1 = \eta_2 = 1$

t_D	p_D
0.10	0.0125
0.30	0.1485
1.00	b.5289
3.00	'1.0077
10.00	'1.589 1
30.00	2.1454
100.00	2.9698
300.00	4.2823
1000.00	6.8497
3000.00	11.0066
10000.00	19.1288
30000.00	3b.2759
100000.00	57.9617
300000.00	W.5366
900000.00	17'1.5466

Fourfirst Program :

$y^{\circ}_D = 20$
skin = 0
a = 6
b = 10
$x_D = 7$
$y_D = 10$
$\lambda_1 = \lambda_2 = \eta_1 = \eta_2 = 1$

t_D	p_D
0.10	0.0125
0.30	0.1485
1.00	10.5289
3.00	1.0077
10.00	1.5891
30.00	'2.1454
100.00	12.9698
300.00	4.2823
1000.00	6.8497
3000.00	11.0066
10000.00	19.1288
30000.00	32.2759
100000.00	47.9617
300000.00	99.5366
900000.00	171.5466

TABLE C-2

Selected Data from Composite Reservoir -- Nonshif'ted

$y^{\circ}_D = 20$
skin = 0
a = 6
b = 10
$x_D = 7$
$y_D = 10$
$\lambda_1 = \lambda_2 = \eta_1 = \eta_2 = 1$

t_D	p_D
0.10	'0.0125
0.30	0.1485
1.00	0.5289
3.00	1.0077
10.00	1.589 1
30.00	2.1454
100.00	12.9698
300.00	4.2823
1000.00	6.8497
3000.00	1 1.0066
10000.00	1 9.1288
30000.00	3 2.2759
100000.00	$7.96 17
300000.00	99.5366
900000.00	17 1.5466

$y^{\circ}_D = 200$
skin = 0
a = 6
b = 10
$x_D = 7$
$y_D = 10$
$\lambda_1 = \lambda_2 = \eta_1 = \eta_2 = 1$

t_D	p_D
0.10	0.1258
0.30	11.4851
1.00	5.289 1
3.00	10.0772
10.00	15.8894
30.00	2 1.3715
100.00	27.4417
300.00	32.999 1
1CCCOO	39.0972
3000.00	44.7439
10000.00	53.0249
30000.00	66.1691
100000.00	91.8554
300000.00	133.4304
900000.00	205.4403

TABLE C-3

Selected Data from Composite Reservoir -- Shifted

$y^{\circ}_D = 20$
skin = 0
a = 6
b = 10
$x_D = 7$
$y_D = 10$
$\lambda_1 = \lambda_2 = \eta_1 = \eta_2 = 1$

t_D	p_D
0.10	0.0125
0.30	0.1485
1.00	0.5289
3.00	1.0077
10.00	1.5891
30.00	12.1454
100.00	2.9698
300.00	4.2823
1000.00	6.8497
3000.00	11.0066
10000.00	49.1288
3m.00	32.2759
100000.00	57.9617
300000.00	49.5366
900000.00	171.5466

$y^{\circ}_D = 200$
skin = 0
a = 6
b = 10
$x_D = 7$
$y_D = 10$
$\lambda_1 = \lambda_2 = \eta_1 = \eta_2 = 1$

t_D	p_D
0.10	0.0125
0.30	0.1485
1.00	0.5289
3.00	1.0772
10.00	1.5889
30.00	2.1371
100.00	2.7441
300.00	3.2999
1000.00	3.9097
3000.00	4.4743
loooO.OO	5.3024
3oooO.00	6.6169
100000.00	9.1855
300000.00	13.3430
900000.00	20.5440

TABLE C-4

Selected Data for Varying Mobility Ratios and Skin

Case 1 : High Mobility Ratio

$y^{\circ}_D = 20$
skin = 0
a – 6
b = 10
$x_D = 7$
$y_D = 10$
$\lambda_1 = 1000$
$\lambda_2 = 1$
$\eta_1 = 12 = 1$

t_D	p_D
3.00	1.0077
10.00	1.5903
30.00	2.2049
100.00	3.4227
300.00	5.7662
1000.00	10.7076
3000.00	18.9139
10000.00	35.0802
3m.00	613 162
100000.00	112.6169
300000.00	1195.6737
1000000.00	357.9572
3000000.00	620.6351
10000000.00	11133.8394

Case 2 : High Boundary Skin

$y^{\circ}_D = 200$
skin = 10000
a – 6
b = 10
$x_D = 7$
$y_D = 10$
$\lambda_1 = \lambda_2 = \eta_1 = \eta_2 = 1$

t_D	p_D
0.10	0.0125
0.20	0.7457
1.00	0.5289
2.00	0.8223
10.00	1.5904
20.00	1.9559
100.00	3.4242
200.00	4.7205
1000.00	10.7351
2000.00	15.3963
10000.00	35.3906
2oooO.00	$0.5535
100000.00	**115.9147**
200000.00	**166.3672**
900000.00	**372.6822**

TABLE C-5

The Line Source Solution

t_D	p_D
0.10	0.0124
0.30	0.1463
0.60	0.3376
1.00	0.5221
3.00	0.9947
6.00	1.3210
10.00	1.5683
30.00	2.1092
60.00	2.4537
100.00	2.7084
300.00	3.2568
600.00	3.6032
1000.00	3.8585
3000.00	4.4077
6000.00	4.7452
10000.00	5.0097
30000.00	5.5590
60000.00	5.9055
100000.00	6.1610
300000.00	6.7103
600000.00	7.0569
1000000.00	7.3122
3000000.00	7.8616
6000000.00	8.2081
10000000.00	8.4635